REPUBLIC OF TÜRKİYE

ALTINBAŞ UNIVERSITY

Institute of Graduate Studies

Electrical and Computer Engineering

DESIGN OF A MICROSTRIP DIPLEXER FOR RECENT WIRELESS COMMUNICATION SYSTEMS

Meena Adnan Jaafar Al-BAGHDADI

Master`s Thesis

Supervisor

Asst. Prof. Dr. Mesut ÇEViK

Istanbul, 2023

DESIGN OF A MICROSTRIP DIPLEXER FOR RECENT WIRELESS COMMUNICATION SYSTEMS

Meena Adnan Jaafar AL-BAGHDADI

Electrical and Computer Engineering

Master`s Thesis

ALTINBAŞ UNIVERSITY

2023

The thesis titled DESIGN OF A MICROSTRIP DIPLEXER FOR RECENT WIRELESS COMMUNICATION SYSTEMS prepared by MEENA ADNAN JAAFAR AL-BAGHDADI and submitted on March/2023 has been **accepted unanimously** for the degree of Master of Science in Electrical and Computer Engineering.

Asst. Prof. Dr. Mesut ÇEViK
Supervisor

Thesis Defense Jury Members:

Asst. Prof. Dr. Mesut ÇEVİK	Department of Electrical and Electronics Engineering, Altınbaş University	____________
Asst. Prof. Dr. Hasan ABDULKADER	Department of Computer Engineering, Altınbaş University	____________
Assoc. Prof. Dr. Özlem ÜNVERDİ	Department of Electronics and Communications Engineering, Yıldız University	____________

I hereby declare that this thesis meets all format and submission requirements of a Master`s Thesis.

I hereby declare that all information presented in this graduation project has been obtained in full accordance with academic rules and ethical conduct. I also declare all unoriginal materials and conclusions have been cited in the text and all references mentioned in the Reference List have been cited in the text, and vice versa as required by the abovementioned rules and conduct.

Meena Adnan Jaafar Al-BAGHDADI

Signature

ACKNOWLEDGEMENTS

Before I thank anyone, I praise Allah, the beneficent and the merciful, for everything in prosperity and adversity.

I want to express my sincere gratitude to all the instructors who taught me more than just science, especially my supervisor Asst. Prof. Dr. Mesut ÇEVİK, for all the time, support, and guidance provided to me along the journey to accomplish this work.

ABSTRACT

DESIGN OF A MICROSTRIP DIPLEXER FOR RECENT WIRELESS COMMUNICATION SYSTEMS

AL-BAGHDADI, Meena Adnan Jaafar

M.Sc., Electrical and Computer Engineering, Altınbaş University,

Supervisor: Asst. Prof. Dr. Mesut ÇEViK

Date: April / 2023

Pages: 78

In recent years, microstrip diplexer filter has gained much recognition, especially in wireless communication systems like mobile phones, radio transmittals, broadband wireless, as well as satellite-based communication systems, due to their ability to combine two separate filters in one device using a communication channel. In this work, a meander line resonator, a steps impedance resonator, and a uniform impedance resonator are used to build a microstrip diplexer using FR4 epoxy laminate material. Mathematical formulas are used in the design process to zero in on the optimal qualities that will allow for fine-tuning the resonant frequency. The meandering structure is proposed to miniaturize the suggested diplexer compared to its original size. High isolation between the output ports is accomplished, as well as the structure maintains a basic topology and small size. From the proposed design, excellent performance characteristics including high isolation, low insertion loss, and good frequency selectivity are all achieved. The proposed design has been created and stimulated using Advanced Wave Research (AWR) has been at 1.94GHz and 2.515GHz for GSM-II, WIFI/WLAN. An FR4 epoxy laminate is used to fabricate the suggested diplexer, and the dimension of $32 \times 26\text{mm}^2$, with an insertion loss of 2.9 dB and a return loss of 31.69 dB; the simulated isolation between both two filters is greater than 25.2 dB. Finally, the design

sample has been implemented by fabrication to verify the simulated results. The fabricated diplexer has been measured using an analyzer VNA (vector network analyzer).

Keywords: Step Impedance Resonator, Microstrip, Isolation, GD, Return Loss, Receive Filter.

TABLE OF CONTENTS

Pages

LIST OF TABLES

Pages

LIST OF FIGURES

Pages

ABBREVIATIONS

AWR	:	Advanced Wave Research
WIFI	:	Wireless Fidelity
WIMAX	:	Worldwide Interoperability for Microwave Access
VNA	:	Vector Network Analyzer
Tx	:	Transmit Filter
Rx	:	Receive Filter
PHY	:	Physical Layer
MAC	:	Media Access Control
SIR	:	Step Impedance Resonator
UIR	:	Uniform Impedance Resonator
BPF	:	Band-Pass Filters
PCB	:	Printed Circuit Board
EV	:	Electronic Warfare
SSIR	:	Symmetrical Step Impedance Resonator
ASSIR	:	A Symmetrical Step Impedance Resonator
IL	:	Insertion Loss
RL	:	Return Loss
GD	:	Group Delay
DCLSIR	:	Dual Closed Loop Stepped Impedance Resonator
FBW	:	Fractional Bandwidths
SIW	:	Substrate Integrated Waveguide
RO	:	Radio Occultation
TZs	:	Transmission Zeroes
ANN	:	Artificial Neural Network
SOLR	:	Squared Open-Loop Resonator
SIW	:	Substrate Integrated Waveguides
MAC	:	Media Access Control
RF	:	Radio Frequency
PHY	:	Physical Layer
EM	:	Electromagnetic

TEM : Transmission Electron Microscopy

LIST OF SYMBOLS

S_{11}	:	Input Scattering Coefficient
S_{21}	:	Transmission Coefficient
L_R	:	Return Loss
L_{Ar}	:	Passband Ripple
Ω_C	:	Angular Cut Frequency
f_0	:	Fundamental Resonant Frequency
ωc	:	Cut-off Angular Frequency
R	:	Input Impedance
C_P	:	Parallel LC Resonator in the Band Pass Filter
C_S	:	Series LC Resonator in the Band Pass Filter
L_P	:	Parallel LC Resonator in the Band Pass Filter
L_S	:	Series LC Resonator in the Band Pass Filter
ω	:	Angular Resonator Frequency
g	:	Element Transformation
C_g	:	Gap Capacitor
f_c	:	Cut-off Frequency
f_1, f	:	Resonant Frequencies
λ_0	:	The Free Space Wavelength
λ_g	:	Guided wavelength
λ_g	:	Half-Wavelength
λg	:	Quarter Wavelength
Z_{ine}	:	Even Input Impedance
Z_{ino}	:	Odd Input Impedance
$Z_0,$	:	Characteristic Impedance
θ	:	Electrical Length
K	:	Impedance Ratio
β	:	Propagation Constant
W	:	Width of Conductor in Microstrip Line
c	:	Velocity of Electromagnetic Waves in Space
l	:	Physical Length of the Microstrip

η	:	Impedance of Free Space
G	:	conductance
Y	:	Admittance
h	:	Thickness of the Dielectric Substrate
ε_{re}	:	Effective Dielectric Constant
ε_r	:	Relative Dielectric Constant
Δf	:	Fractional Bandwidth
σ	:	Conductive Losses
μo	:	Permeability of Vacuum
αc	:	Conductive Losses
αd	:	Dielectric Loss
V_P	:	Phase Velocity
tan	:	Loss Tangent
τ_D	:	Group Delay
Q	:	Quality Factor
C	:	Capacitance
L	:	Inductor
R	:	Resistance
GS	:	conductance
Gr	:	Radiation Conductance
δs	:	Skin Depth
μ	:	Permeability
a	:	Loss Coefficient (Attenuation)
η	:	Impedance of Free Space
t	:	thickness
ε	:	Electric Permittivity
$\mathrm{C_a}$	:	Capacitance
C_d	:	Capacitance
α_d	:	Conductor loss
ϕ_{21}	:	Radians Angular Resonator Frequency

1. INTRODUCTION

1.1 RESEARCH BACKGROUND

Microwave filters, which enable frequency selectivity in satellites, mobile communications, radar, and other types of contemporary communication systems, are vital components of current communication systems. Generally, diplexer and multiplexer are microwave filters used to channel signals of different frequencies. In fact, a set of filters and a common junction combine to form a passive multiport device which is known as a multiplexer. The primary role of a multiplexer is to segregate or combine signals from several frequency bands. In fact, a multiplexer is a passive multiport device made up of a series of filters and a common junction. The primary role of a multiplexer is to segregate or combine signals from several frequency bands. The former is the simplest form of a multiplexer. In recent years, diplexer has gained much recognition, especially in wireless communication systems such as cellular networks, broadband wireless, satellite, and radio, because it is able to combine two distinct filters into a single device using communication channels. To illustrate, the microwave diplexer enables two transmitters to share one antenna with low interference between signals. Therefore, a device's weight and size are decreased by having a single antenna. As a result of the growth and development of standards, many innovations in both diplexers and multiplexers technologies have emerged. In fact, a diplexer is used to combine two antennas operating on different frequencies into one common port. A brief overview of diplexer applications will be included in this chapter.

1.2 DIPLEXERS APPLICATIONS

Wireless communication systems have been introduced, and they have made significant progress during the last years, been rapidly developed, and wireless internet, such as Wi-Fi and WiMAX, mobile wireless communication systems, and 3G, 4G, and 5G innovations have also been developed. As a result of these fast advancements, more robust radio frequency components were needed. At this point in time, satellite systems have shifted their focus away from static communications and toward remote sensing, navigation implementations, and mobile applications [1].

As most communication systems demand lightweight, low-cost, high reliability, and higher frequency electronics, diplexer has become a core component in many communication systems. As seen in (Figure 1.1), the application of diplexer technology is quite commonplace in radio base stations as well as radio devices.

To allow for the use of a single antenna in the broadcast and receive paths of two distinct frequency bands, a diplexer is equipped with three ports. In fact, can be described as a device that has three ports, which are used to combine two networks into a single, shared port [2]. Therefore, the diplexer is less expensive than other devices that connect through separate channels [3].

The diplexer can be used as a transmitter or receiver, and it also features an antenna port [4]. In addition, it consists of a power divider as well as two filters meeting standard standards for selectivity and isolation. Both filters are coupled to their respective ports; one at the transmitter's end and the other at the receiver's. The antenna and the two filters are linked via the third port [5].Filters have to have a small failure of insertion and a significant loss of return for robust impedance matching of high-frequency selectivity and connector components. This is necessary to prevent interference. If the filter has a high-frequency selectivity, then it can be established that the guard band between each channel is low, which determines that the frequency can be used effectively[6]. In recent years, designers have been working with a variety of various topologies in an effort to develop microstrip diplexers for use in contemporary microwave transceivers [7].

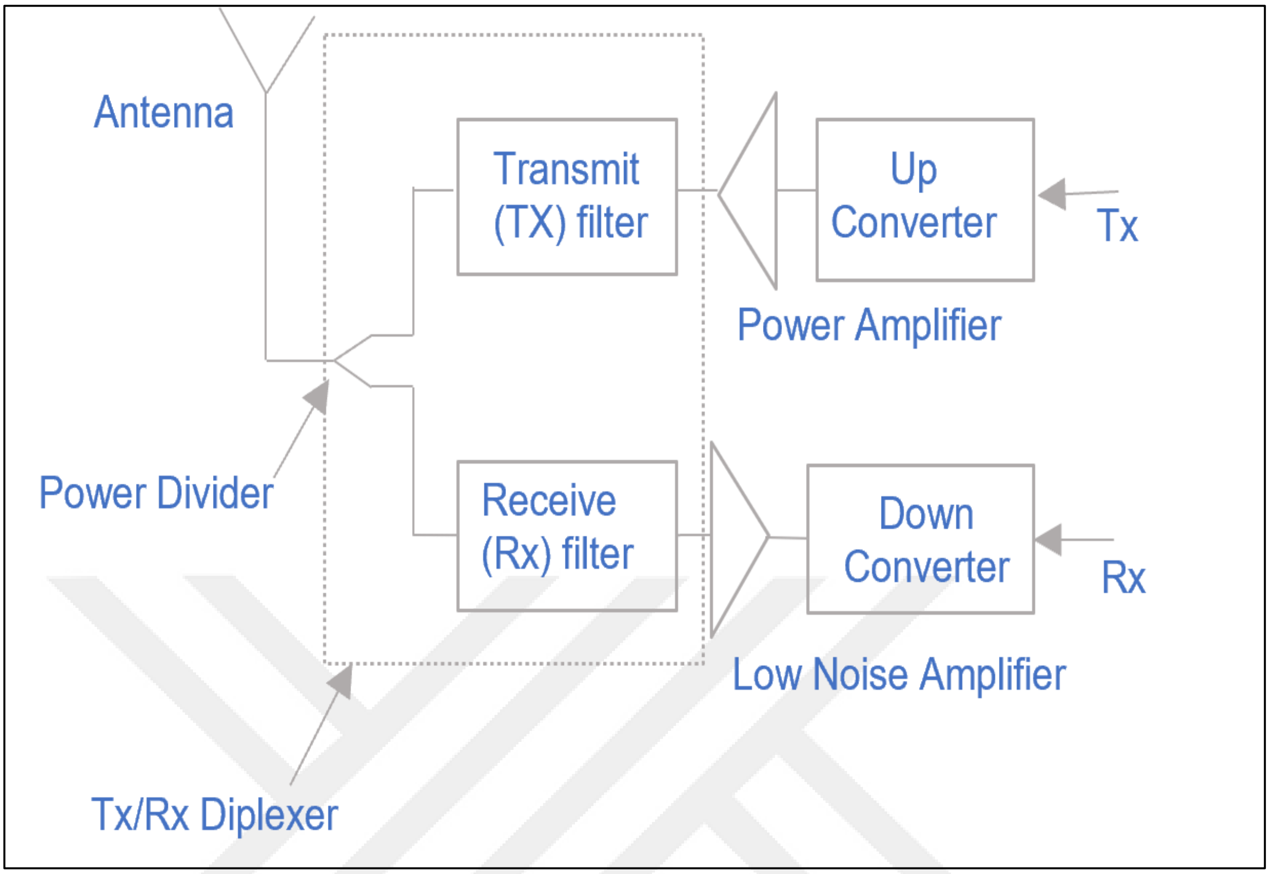

Figure 1.1: Utilization of Diplexer Technology in Base Stations.

There is a comparison between diplexer and duplexer, it will be included as follows in Table 1.1:

Table 1.1: The Difference Between Diplexer and Duplexer.

<table>
<tr><th>Diplexer</th><th>Duplexer</th></tr>
<tr><td>Diplexer is a 3-port RF device that offers two signal pathways to be used on the same antenna or transmission line.</td><td>3-port RF device, splits antenna signals into two channels based on direction.</td></tr>
<tr><td>The diplexer works well with large frequency ranges.</td><td>The frequency bands will possess very nearer frequency bands.</td></tr>
<tr><td>Used in telecommunications, where various modulation schemes and carriers share the same antenna.</td><td>A duplexer can be used in radar and radio communication systems where the high-power transmitter signals need to be isolated but operate on the same antenna.</td></tr>
<tr><td>
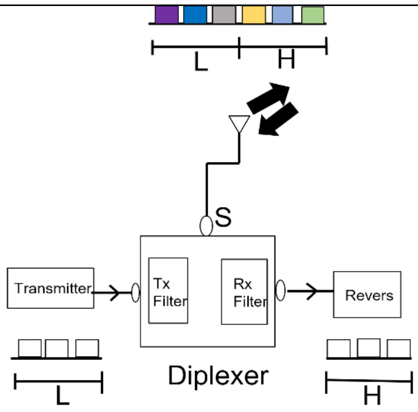

</td><td>
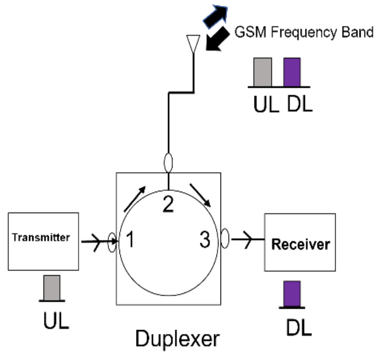

</td></tr>
</table>

1.3 THE STANDARDS OF WLAN SYSTEMS

A WLAN is a computer network that uses wireless distribution to link together two or more devices in a contained space, like a home, business building, or educational institution. Users need to be physically present inside a particular coverage area in order to make advantage of this. The IEEE 802.11 standards, developed by the Institute of Electrical and Electronics Engineers, are the basis for modern WLANs. These standards are more often referred to as “Wi-Fi”.

WLAN communication is enabled thanks to IEEE 802.11's Physical Layer and Media Access Control protocols operating in the 5, 3.6, 2.4, as well as 60 GHz frequency bands. These bands cover a total of 80 GHz. The IEEE 802 standards committee is in charge of their creation and maintenance. Since the first publication of the standard in 1997, which was followed by a number of updates after its initial release.

The IEEE 802.11 family of modulation technologies all make use of the same protocol for their half-duplex through-the-air transmissions. Although the IEEE 802.11-1997 standards were the first of their kind, widespread adoption did not occur until the release of the 802.11 b specification. Information about the IEEE 802.11 family of standards is summarized in Table 1.2.

Table 1.2: The Family of IEEE 802.11 Standards Is Presented.

Electrical and Electronics Engineers (IEEE) 802.11	Frequency (F)	Max Speed (MS)	Compatible
802.11-(a)	5 Gigahertz	54 Mbit /s	Non
802.11-(b)	2.4 Gigahertz	11 Mbit /s	Non
802.11-(g)	2.4 Gigahertz	54 Mbit /s	802.11-(b)
802.11-(n)	2.4 Gigahertz, 5 Gigahertz	600 Mbit /s	802.11-(a/b/g)
802.11-(ac)	5 Gigahertz	1.3 Gbit /s	802.11-(b/g/n)

1.4 AIM OF THE WORK

Microstrip diplexers for cutting-edge microwave transceivers have been the focus of numerous research efforts in recent years, by applying a variety of structures. Nevertheless, several other diplexers with high insertion losses and considerable size requirements have been presented.

a. The goal of this study is to develop a compact, low-cost microstrip diplexer with good performance characteristics such as isolation, insertion loss, and frequency selectivity.
b. The suggested diplexer employs a step impedance resonator (SIR), a uniform impedance resonator (UIR), as well as meander lines to perform the necessary tasks.
c. Within this work, a new geometrical structure has been introduced with benefits in terms of reduced size and lower insertion losses at both band-pass filters (BPF).

1.5 THESIS ORGANIZATION

a. Chapter one: This chapter discusses the background of the study. Problems are identified as well as the main objectives that are to be achieved throughout the study.

b. Chapter two: This chapter introduces a theoretical background regarding the design and formulation of microstrip diplexer in chronological order. Also, the main design components for diplexer are defined in a detailed description.
c. Chapter three: This chapter includes a complete account of all the steps used to design the proposed diplexer as well as the materials. Diplexer is created using the step impedance resonator, uniform resonator, and meander line resonator.
d. Chapter four: In this chapter, the result is presented, and discussed. Also, the proposed diplexer has been created and compared with previous studies. Besides, the simulation work has been improved.
e. Chapter five: This chapter introduces the conclusions and future aspects of the study.

2. LITERATURE REVIEW AND THEORY

2.1 INTRODUCTION

This chapter's reported works will be provided in the literature section. Additionally, a detailed description of the basic components used with regards to the construction of the microstrip diplexer.

2.2 WORK RELATED

The development of the microstrip-antenna concept started during the 1970s with the increase of research publications on the concept by many worldwide scholars [8]. The rapid growth in wireless communication applications causes new microstrip antenna designs to be established to reach high performance in modern communication systems. In modern communication systems, filters and diplexers play major and essential roles. A well-designed diplexer should be reasonably priced and highly effective in performance. The conventional method for creating microstrip diplexers involves first creating two separate filters, then creating a marching circuit. Combining two band-pass filters (BPFs) is the most intuitive approach [9]. Microstrip diplexer is designed to have been widely used in many wireless communication applications. Several structures have been suggested in the design and formulation of diplexer will be stated below:

There are several approaches in the construction of RF diplexers based on different filter configurations [10], but three of them are frequently applied:

a. Two band-pass filters are used, each with a different center frequency.
b. The application of a band-pass filter for one channel and a band-stop filters for the other channel that rejects the same frequency band.
c. The application of two center-frequency-different band-stop filters.

In each diplexer, two channels are working at two frequencies for specific applications. For instance, in 2019, Abbas Rezaei et al [11]. proposed a diplexer that was designed for WiMAX technology and wireless applications, while the designed diplexer by Salah I. Yahya et al., in 2019 was created for frequency division duplex and GSM-4G applications [12].

In 2018, Qun Li et al., [13] proposed a high-isolation microstrip diplexer filter that was invented using a feeding line coupling technique based on a short stubs-load resonator to generate transmission zero at a lower frequency. It operates on two channels at 3 and 5 GHz for wireless applications that require a high level of isolation.

In 2019, Saif N. Dembele et al., [14] it has been proposed that a tiny microstrip diplexer that is based on a dual closed-loop stepped impedance resonator (DCLSIR) might be used. The microstrip diplexer that has been presented is put together using a combination of two DCLSIR bandpass filters (BPFs). Compact in size, the diplexer that was constructed operates at 8.3/10 GHz.

In 2020, Salah I. Yahya et al., [15] proposed a planar dual-channel bandpass microstrip diplexer a new structure for design. It has a very compact size, measuring just $0.0081\lambda_g^2(9\ \mathrm{mm}^2)$ and it was constructed on a dielectric substrate that is 0.787 mm in height. The suggested diplexer is suitable for use in broadband applications due to its wide fractional bandwidths (FBWs%), which come in at 34.3% for the first channel and 38.6% for the second channel respectively. The L-band resonance frequencies are found at $f_1 =$ 1.6GHz, and the WiMAX resonance frequencies are located at $f_2 = 3$GHz.

In 2020, Abbas Rezaei et al., [16]proposed a microstrip diplexer designed to work at frequencies of 0.78 GHz and 1.85 GHz, based on the patch and thin cells, and intended for use in GSM applications. Due to the fact that the suggested resonator has a symmetrical construction, both the odd and even modes studies are carried out in order to get information regarding the behavior of the resonator. The newly developed diplexer offers a number of advantages, including good isolation, low insertion losses, and low return losses. Additionally, its size is rather compact.

In 2020, Nrusingha Charan Pradhan et al., [17] proposed a novel small substrate integrated waveguide (SIW) diplexer for C-band applications with square cavities. This diplexer employs evanescent-mode propagation below the cutoff frequency of the cavity. When centered at 6.16 GHz and 7.72 GHz, the lower and higher passbands have insertion losses of 0.83 dB and 0.77 dB, respectively. The suggested diplexer offers 22 dB of isolation and a fractional bandwidth of 5.1% for each passband.

In 2020, Trushit Upadhyaya et al.,[18] an innovative microstrip diplexer with high isolation and a tiny electrical compact has been created, for the Radio Occultation (RO) System that will be used in future planetary systems, The method of radio occultation is being used widely in order to investigate many aspects of the atmospheres of planetary systems. The properties of a planet's atmosphere are being studied in great detail using the radio occultation method. The frequency synthesizers are utilized within the On-board RO transmitter, which operates within two distinct frequency bands, at 6.7 GHz, and 8.4 GHz frequencies.

In 2020, Qing-Yuan Lu et al.,[19]Microstrip diplexers with several transmission symmetries are expected to become commercially available. (TZs) Uniform impedance resonators (UIRs) operating at 0.755 GHz and 1.056 GHz using shared element loaded UIR are used, and this has benefits for the Global System for wireless communication (FDD).

In 2021, Salah I.Yahya et al. [20]proposed an artificial neural network (ANN) used to design and construct a high-performance microstrip diplexer. input frequency, substrate type, substrate thickness, and physical dimensions are incorporated into the ANN model. This model generates S-parameters and group delay values (GD). The multilayer perceptron neural network trained with backpropagation operates between 1.4 and 3 GHz.

In 2021, CHI-FENG CHEN et al.,[21] an innovative circuit model has been developed, for the purpose of designing multifunction integrated diplexers with frequency division, frequency selection, and power division functionalities. The suggested highly integrated multifunctional diplexer is primarily made up of only two multimode resonators that operate at separate frequencies and two isolation resistors. The distributed coupling method was utilized in order to combine the two multimode resonators. The passband of a channel was created using a single resonator. Responses for second order and third-order filtering were made.

In 2022, M.M. SHAHEEN et al.,[4], [22] proposed a microstrip diplexer based on a squared open-loop resonator (SOLR), including its design and hardware implementation. In order to construct a bandpass filter with a high level of selectivity, we made use of four SOLRs, pair of a couple of which were linked with (BPF). In order to put together the suggested diplexer, the BPFs that have been built are connected to one another by a T-junction combiner that has been customized to fit the two filters as well as the antenna port. The suggested diplexer has two resonance frequencies, 1.81 GHz and 2.03 GHz, and these correspond to the transmit and receive modes, respectively.

In 2022, Mehdi chemseddine Farah et al.,[4] proposed a small microwave diplexer design based on the use of a stepped impedance resonator in its construction (SIR). Used in 4G applications, the diplexer is built with two band-stop filters that operate at frequencies of 2.5 and 1.8 GHz. The dimensions of the SIR and the locations of the feeder lines are decided based on the theoretical design and modeling. As the substrate material, FR-4 is utilized. This material has a thickness of 1.6 millimeters and a dielectric permittivity of 4.4.

In 2022, Dongdong Ma et al.,[23] proposed two miniaturized substrate-integrated waveguides (SIW) diplexers based on the orthogonal dual-mode method are proposed. These diplexers have a wide stopband and good isolation. Through the utilization of orthogonal dual-mode SIW junction-resonators in place of the more conventional T-junctions, inter-channel isolations were accomplished for SIW diplexers. In addition, the fractional bandwidth, or FBW, diagrams are applied to make the identification of the possible FBWs in both passbands as simple as possible. Both 12 and 14 GHz are catered to by the two distinct kinds of SIW diplexers.

In 2022, Abbas Rezaei et al.,[24] proposed a compact microstrip diplexer for modern wireless communication system applications using two BPFs. In order to reduce the size considerably, the shunt stub is inserted within the U-shape cell that the coupled lines and transmission line form, resulting in the overall size of the given diplexer that is just $0.008\lambda g^2$. The first resonance frequency is equal to 895 MHz, while the second resonance frequency is equal to 2.2 GHz.

Table 2.1: Provides a Summary of the Articles That Were Quoted Before, in Addition, the Specifications for Each Design That Was Offered are Outlined.

Ref	year	Technology	Size $mm^2/\ \lambda_g^2$	Application	f_{01}, f_{02} (GHz)	FBW1, FBW2 %	IL1, IL2 (dB)	RL1/RL2 (dB)	Isolation (dB)
[11]	2019	Coupled lines	0.028	WiMAX And wireless applications	2.88/3.29	----	0.36/0.44	23.7	23
[12]	2019	Coupled lines	0.047	frequency division duplex and GSM-4G applications	2.85/2.72	----	0.85/0.8	15.7/24	21
[13]	2018	Distributed coupling feeding line	0.29 × 0.18	For WiMAX and WLAN applications	2.95/4.92	12.8/9.3	1.47/1.4	16/28	40
[14]	2019	Dual Closed Loop Stepped impedance resonator	0.65 × 0.11	For X-band application	8.3/10	11/13	1.8/1.9	10/10	26
[15]	2020	Coupled stub-loaded U-shape resonators	0.0081	Broadband wireless applications	1.6/3	34.3/38.6	0.45/0.6	27/24	20
[16]	2020	Coupled spiral cells	0.026	For GSM	0.78/1.85	-	0.17/0.3	19/21	42

				and WLAN application					
[17]	2020	Compact substrate integrated waveguide (SIW) diplexer	0.88	For C-Band applications	6.16/7.72	5.19/5.44	0.83/0.77	20/20	22
[18]	2020	Step impedance resonators and patch-resonators	0.52 × 0.625	Radio science planetary applications	6.7/8.4	4.6/4.34	0.68/0.82	27.68/31.02	27
[19]	2020	Uniform impedance resonator (UIR)	0.29 × 0.14	FDD	1.056/1.214	------	1.1/2.2	-----	24
[20]	2021	(ANN) Backpropagation	0.004	L-band S-band Energy harvesting applications	1.4/3	47/45	0.006/0.07	28.6/20	20
[21]	2021	Distributed coupling	53.5 × 31.7 0.098	Rf and multiband communication	1.525/2.125	3.7/3	4.2/4.6	17/23	23
[22]	2022	SLOR And T-Junction	1.5	Wireless application	1.81/2.03	2.25/3	1.98/1.9	34.6/26	58
[4]	2022	Stepped Impedance Resonator	9350.63	For 4G applications	1.8/2.5	10.5/7.6	2.69/2.81	19.19/15.54	17
[23]	2022	Dual-mode technique SIW diplexer	3.47 3.62	Stopband wireless applications	12/14 12/14	2.04/2.44 3.73/3.99	2.51/2.19 1.39/1.37	20/20 20/20	22 47

[24]	2022	Coupled lines	0.008	Wireless application	0.895/ 2.2	31/31	0.075/ 0.14	40.3/31.7 7	21

2.3 THE COMPONENT DESCRIPTION

2.3.1 Transmission Line

A transmission line is an enclosed system that transmits energy from one location to another. It includes coaxial cables, waveguides, and other systems of conductors that are used to move electrical signals from one destination to another. Transmission lines are specially designed for transmitting electromagnetic waves. As shown in figure (2-1) microstrip lines are one of the most common types of planar transmission lines because they are easy to make smaller and easy to connect to other passive and active microwave devices [25]. Photolithographic methods can also be used to make them. Microstrip lines can be used with a wide range of substrate materials and work at high frequencies [26].

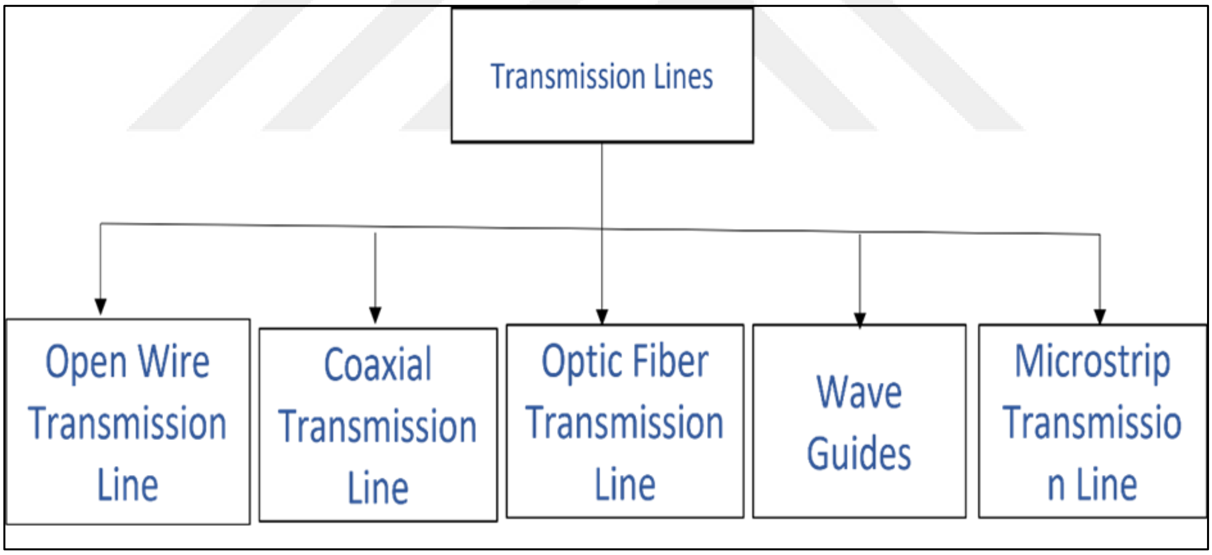

Figure 2.1: Types of Transmission Lines.

2.3.2 Microstrip Transmission Line Structure

Microstrip is used to make low-cost, compact, and simple-to-integrate microwave circuits. As depicted in (figure 2-2), a microstrip transmission line consists of a conductor with three layers: the top layer consists of a conducting strip and is designated by the symbols W (width) and t (thickness). In the process of creating the circuit design for the microstrip structure, this layer plays an important function. A dielectric substrate layer makes up the intermediate layer of the structure. This layer is characterized as having a height of h and a thickness of ε_r (dielectric constant). A ground plane is the lowest layer. Moreover, the microstrip structure is a "printed circuit board", or PCB for short. This type of board is utilized in the manufacture of fabrication microwave tools. As a result, the filter can be built utilizing either a microstrip structure or a planar resonator as the foundation. With a microstrip arrangement, conductor loss, dielectric loss, and radiation loss are the most likely causes of power losses [27]. Since the fabrication of microstrip lines is based on small-size, lightweight, and low-cost components, it has been used extensively in satellite airborne communications and Electronic Warfare (EV) systems.

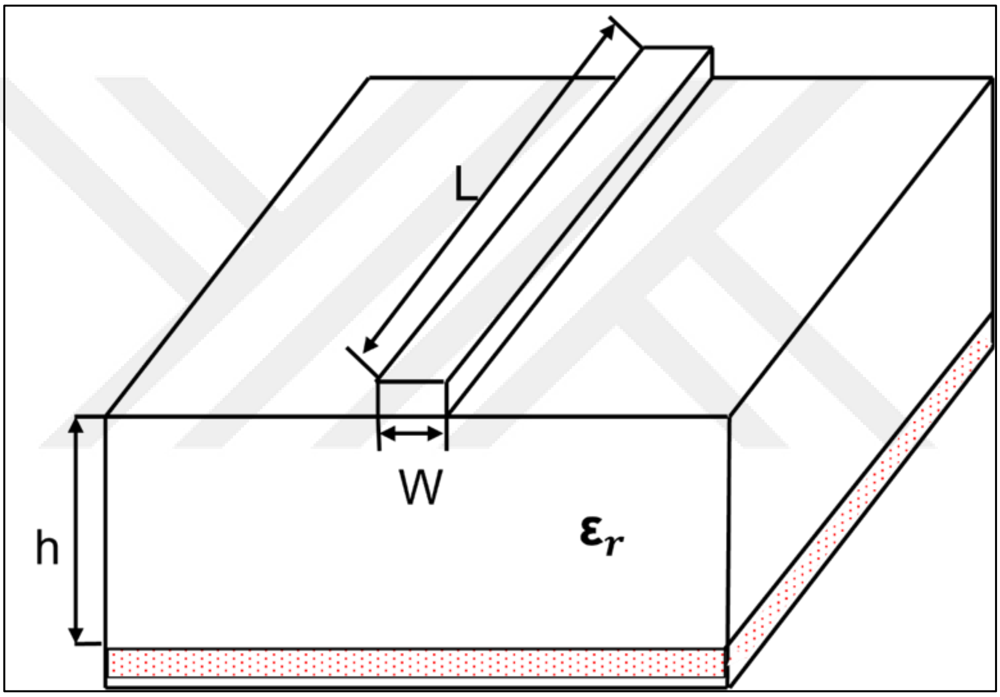

Figure 2.2: General Design of Microstrip Line.

The microstrip structure is not homogenous since both the electric and magnetic fields pass through two different substances, which are the dielectric substrate and the air. Due to the structure's inhomogeneity which makes components for both fields to flow in the same direction, there is no pure TEM mode in a microstrip line. The reason for that can be contributed to the fact that there are two guided media with distinct magnetic permeabilities (μ) and electric permittivity (ε). In this case, the wave propagation is (wave travels in two mediums), therefore, the propagation velocity will be determined by the features of the two media (ε" and " μ) by the physical dimensions of the microstrip structure. In comparison to the transverse components, the electric and magnetic field components in the direction of propagation for the dominant mode in the microstrip line are so tiny as to be deemed unimportant. This behavior, which resembles that of the TEM mode, is referred to as the "quasi-TEM approximation". It is compatible with the microstrip line.

2.3.2.1 Characteristic impedance

Characteristic impedance (Z_0) is the most significant parameter for any transmission line since it offers wave propagation properties through the interconnection [28]. In fact, the most typical definition of the characteristic impedance of a transmission line is the one defined in terms of field quantities along a transverse cross-section [29]. Following the findings of the quasi-static analysis, the pure TEM mode is identified as the primary mode of wave propagation in the microstrip line. Because of this, the characteristic impedance, denoted by the symbol Z_0, is written as an expression in terms of two capacitances:[30]

$$Z_0 = \frac{1}{c\sqrt{C_a C_d}} \tag{2.1}$$

where C_d is the capacitance of the substrate measured in units of length, C_a is the capacitance of the substrate measured in units of length when exchanged by air, and c is the velocity of the electromagnetic wave while it is moving through space. Several solutions exist depending on the value of W slash and are a function of the width-to-height (H/W) as well as the height-to-width (W/H) ratios of the transmission line. This allows us to determine the microstrip's characteristic impedance at zero frequency (Z_0) [30]:

When, $\left(\frac{W}{H}\right) \leq 1$

$$Z_0 = \frac{60}{\varepsilon_{eff}} ln\left(8\frac{W}{H} + 0.25\frac{W}{H}\right) \tag{2.2}$$

And when, $\left(\frac{W}{H}\right) \geq 1$

$$Z_0 = \frac{\eta}{2\pi\sqrt{\varepsilon_{re}}} \ln\left(\frac{8h}{W} + 0.25\frac{W}{h}\right) \tag{2.3}$$

Where $\eta = 120\pi\Omega$ is the wave impedance in free space.

$$Z_0 = \frac{120\pi}{\sqrt{\varepsilon_{eff}} \times \left[\frac{W}{H} + 1.393 + \frac{2}{3} ln\left(\frac{W}{H} + 1.444\right)\right]} \quad (2.4)$$

If the strip conductor is very thin t→0, the characteristic impedance (Z_0) terms are accurate to more than 1%.

2.3.2.2 Effective dielectric constant

Due to inhomogeneity non the dielectric medium, the distribution of the electromagnetic field (EM) presents a challenge for microstrip lines in the form of the quasi-TEM mode. Since microstrip Lines have been a popular choice in RF circuits, there is always a requirement to obtain the effective dielectric constant (ε_{re}) to study the behavior of EM fields. It is found to depend on the dielectric, including the substrate material, and the width-to-height ratio of the microstrip line. Microstrip's effective dielectric constant can be determined using via[27] :

$$\varepsilon_{re} = \frac{C_d}{C_a} \quad (2.5)$$

where C_d is the capacitance of the substrate measured in units of length, C_a is the capacitance of the substrate measured in units of length when exchanged by air, and c is the velocity of the electromagnetic wave while it is moving through space.

When, $\left(\frac{W}{H}\right) < 1$

$$\varepsilon_{re} = \frac{\varepsilon_r + 1}{2} + \frac{\varepsilon_r - 1}{2}\left[\left(1 + 12\left(\frac{H}{W}\right)\right)^{-1/2} + 0.04\left(1 - \left(\frac{W}{H}\right)\right)^2\right] \quad (2.6)$$

When, $\left(\frac{W}{H}\right) \geq 1$

$$\boldsymbol{\varepsilon_{re} = \frac{\varepsilon_r + 1}{2} + \frac{\varepsilon_r - 1}{2}\left(1 + 12\left(\frac{H}{W}\right)\right)^{-1/2}} \quad (2.7)$$

2.3.2.3 Measurements of electrical length, phase speed, propagation constant, and guided wavelength:

The wavelength of the microstrip's guided quasi-TEM mode can be computed after its effective dielectric constant has been measured following Equation:

$$\lambda_g = \frac{\lambda_0}{\sqrt{\varepsilon_{eff}}} \tag{2.8}$$

The wavelength in open space at the operating frequency f is denoted by λ_0. If you know the frequency in gigahertz (GHz), you may convert it to millimeters (mm) by using the formula below to determine the guided wavelengths by the following Equation:

$$\lambda_g = \frac{300}{f\sqrt{\varepsilon_{eff}}} \tag{2.9}$$

Phase velocity V_p and the associated propagation constant can be evaluated by:

$$\beta = \frac{2\pi}{\lambda_g} \tag{2.10}$$

$$v_p = \frac{\omega}{\beta} = \frac{c}{\sqrt{\varepsilon_{eff}}} \tag{2.11}$$

The electric length for a given physical fixed length of microstrip is defined as follows Equation, where c is the speed of light ($c = 3 \times 10^8 \text{meter/second}$) in free space.

$$\theta = \beta l \qquad 2.12)$$

Thus, $\theta = \pi$ when $l = \lambda g/2$, and $\theta = \pi/2$ when $= \lambda g/4$, While developing microstrip filters, these so-called quarter-wavelength, as well as half-wavelength microstrip lines, are crucial components.

2.3.3 Microstrip Losses

According to [31] the factors contributing to microstrip line loss are:

a. Loss of conductor
b. Loss of dielectric
c. Loss of radiation
d. Propagation of surface

The first two types of losses are known as dissipative effects, while the latter two types of losses are known as parasitic events. As a consequence of this, for the purpose of calculation, the losses that are brought on by the conductor and the dielectric may be combined and integrated to provide the attenuation coefficient (α). The dominant microstrip mode's attenuation constant is influenced by geometrical features, the electrical characteristics of the substrate and conductors, as well as by the frequency. To illustrate, Attenuation in a microstrip line is easily represented as a decibel per meter of line length and is defined as the product of the characteristic impedance of the line, Z_0, and the radio frequency resistance per meter, R'. Yet, in everyday use, you might find it more convenient to represent an in terms of (dB) per unit length:

$$\alpha_c = (20log_{10}\ e)\alpha \approx 8.8686\alpha \ (N/U) \tag{2.13}$$

2.3.3.1 Conductor loss

Conductor loss was first investigated by Pucel et al. and later by Wheeler [32]. In fact, conductor losses are greater than the other losses included in microstrip circuits. The attenuation due to conductor loss can be easily calculated with the following formula:

$$\alpha_c = \frac{8.686R_s}{Z_cW} \text{ dB/Unit length} \tag{2.14}$$

Characteristic impedance, denoted by Z_C, is a function of microstrip width, W, and surface resistance, denoted by R_S, is expressed in ohms per square and applies to both the strip conductor as well as a ground plane. According to a conductor:

$$R_s = \sqrt{\frac{\omega\mu_0}{2\sigma}} \tag{2.15}$$

Where μ_0 reflects the permeability of free space, σ is the conductivity, and ω is the angular frequency.

2.3.3.2 Dielectric loss

The dielectric loss in microstrip is a crucial parameter in designing hybrid integrated circuits that need small attenuation [33]. The term (dielectric losses) refers to the interaction between a dielectric material and the electromagnetic field. If the loss tangent of the dielectric substrate and the distribution of the electric field inside the substrate is determined, this loss can be calculated [33]. The attenuation of the dielectric loss in the microstrip can be calculated through the:

$$\alpha_d = 8.686\pi \left(\frac{\varepsilon_{eff} - 1}{\varepsilon_r - 1}\right)\frac{\varepsilon_r}{\varepsilon_{eff}}\frac{tan\,\delta}{\lambda_g} \tag{2.16}$$

Most of the substrates have $\varepsilon_{\mathrm{reff}} \approx \varepsilon_r$ and $\alpha_D \approx 8.686\pi\ ta\,n\,\delta$. The term tan δ is mostly 10^{-3} or less, which means that the dielectric loss is almost 0.027dB/guided wavelength.

2.3.3.3 Radiation loss

Several asymmetric transmission lines of varying types are included in the microstrip structure. This structure may commonly be discovered in an unprotected environment. It consists of several discontinuities, each of which emits a certain quantity of power. Since these discontinuities are so important to the structure of the microstrip, it is impossible to find a suitable replacement for them[31]. They are also recognized as a common irritant. Radiation and surface-wave propagation are both represented by a parallel admittance at the discontinuity's end. This admittance is defined as:

$$Y = G_r + G_s + jB \tag{2.17}$$

where G_r represents the radiation conductance, G_S represents the surface wave propagation conductance, and B represents the susceptance that is the result of the numerous field influences that surround the discontinuity.

2.3.3.4 Propagation of surface

Surface waves exist underneath the dielectric surface, and they are able to propagate away from discontinuities. For frequencies up to 10 GHz, Gr is significantly larger than Gs. On the other hand, Gs starts to make a noticeable difference when the frequency is increased. There are a few steps that might be taken in order to cut down on radiation losses [3].

a. A little piece of absorbent material that is positioned near discontinuities.
b. Making use of confined planar structures of a tiny scale.
c. Utilizing small, enclosed planar structures.
d. Managing the current density that goes through the corners of metallic components of a microstrip structure to steer current flow toward the structure's center.

2.3.4 Microstrip Resonator

With the diplexer's essential role in modern communications, engineers have come up with increasingly creative designs and more refined methods of design to handle the growing complexity of these systems. Diplexers are commonly used in multiservice as well as multi-band communications, and they must be built to fulfill certain criteria. However, in the conventional approach of diplexers, many external junctions led to a more complex and larger size of diplexers. Hence, many different layouts have been developed to meet these needs. For instance, to reduce the circuit size and achieve high performance, different types of resonators, such as open-loop, SIRs, spiral inductor resonators, and meander lines, have been inserted in diplexers[3]. Basically, a resonator is an element that can store both magnetic and electric energy at specific frequencies, with capacitor C holding the electric energy and indicator L storing the magnetic energy.

2.3.4.1 Step impedance resonator and uniform impedance resonator

Step impedance resonators are made up of many transmission lines with various levels of admittances. Filter spurious response as well as insertion loss can be controlled by adjusting the inductance ratio of the stepped impedances. Because of their low price and straightforward structure, SIRs have found the most widespread application in RF and microwave simulations. SIRs are the basic resonant element that can function from RF to millimeter-wave frequencies. They have high Q-factor and compactness; thus, they have been used in filters and oscillators. In addition, SIRs were developed to overcome drawbacks like limited design parameters, spurious responses of uniform impedance resonator (UIR), and Capacitor loaded UIR [34]. Compared to uniform impedance resonators (UIR), widely used in RF and microwave devices, SIRs are smaller in size as well as they can restrict higher frequencies [35]. Examples of UIR and SIR are shown in (Figure 2.3). The UIRs and SIRs configurations will have the same ABCD matrices. However, the physical length of the SIR line will be shorter than that of the UIR line [35]. The matrix can be written as:

$$\begin{bmatrix} A & B \\ C & D \end{bmatrix} = \begin{bmatrix} \text{Cos } \theta & jZ_0\text{Sin } \theta \\ jZ_0^{-1}\text{Sin } \theta & \text{Cos } \theta \end{bmatrix} \qquad (2.17)$$

Z_0 symbolizes the resistance as well as θ symbolizes the length of the UIR line. Replacing the matrix with three matrices at each node in the SIR topology provides more design parameters than uniform-impedance resonator topologies. Therefore, SIR topologies can incorporate this matrix to enhance their performance. On the other hand, The UIR topologies depend on the length of the line to achieve resonance. The SIRs resonance state is significantly affected by length ratio as well as impedance ratio. These factors are significant as they help to understand the behavior of SIRs in UIR topologies, which are often utilized in the design of microwave filters. Here is an expression of the resistance to the SIR:

$$K = tan\ \theta 1 tan\ \theta 2 \qquad 2.18)$$

Where " K " is the coefficient for the impedance ratio equal to Z_2/Z_1 . However, $\theta 1$ and $\theta 2$ represent electrical lengths in the SIR. It is known that the electrical length of a resonator is shortest for $0 < K < 1$ and longest for $K > 1$. High discontinuity in SIR has been seen for very large K , leading to poor insertion loss [35].

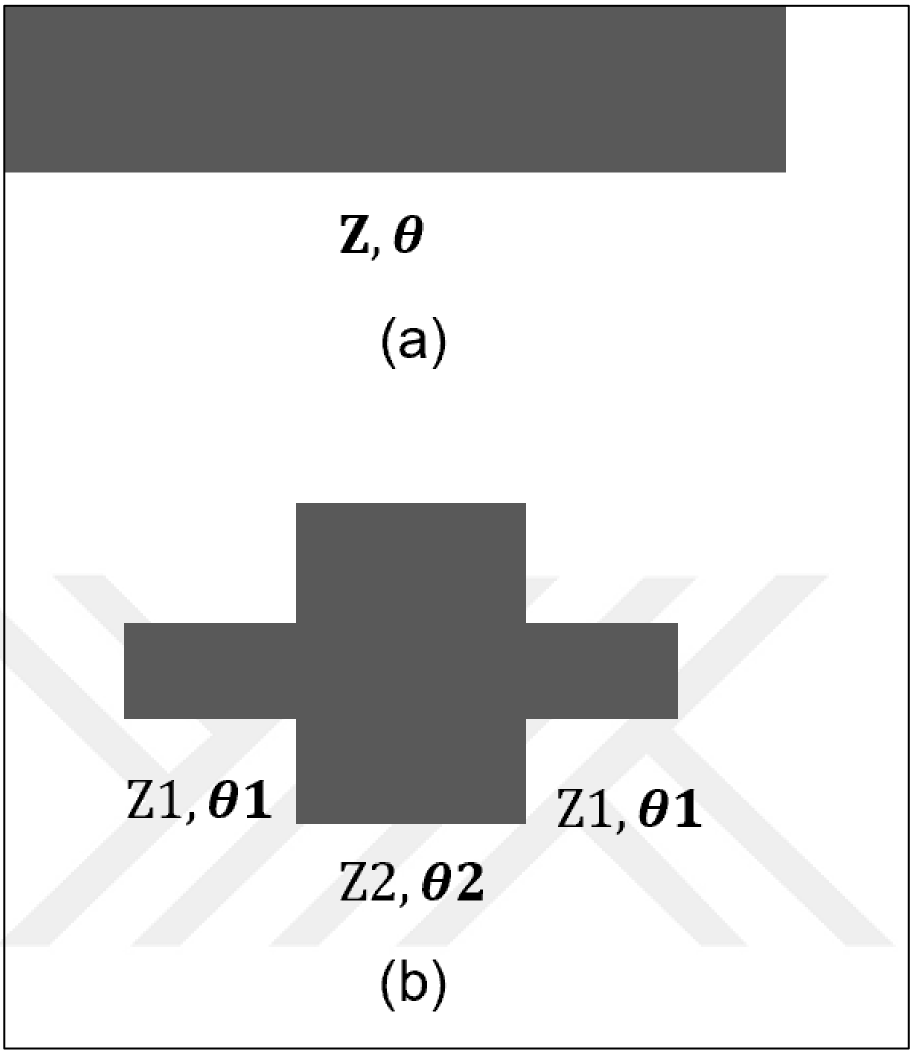

Figure 2.3: Step Impedance Resonator Equivalent to The UIR.

There are two unique kinds of SIRs, those with symmetric (SSIR) structures along with asymmetrical (ASIR) structures, as depicted in Figure (2-4). In SIR structures, it is well known that the microstrip section with the narrower width has a greater resistance compared to the one with the wider width. symmetric SIR occurs when $Z1 < Z2$, and asymmetric SIR occurs when $Z4 > Z5$. Electrical lengths are accordingly designated by d1 as well as d2 for symmetrical SIR and e1 as well as e2 with asymmetrical SIR. Generally, symmetrical SIR consists of three-step resistance sections of equivalent electrical length plus end-to-end impedance symmetry. The impedance ratio of the symmetrical SIR stands in for the SIRs dimensions condition (K).

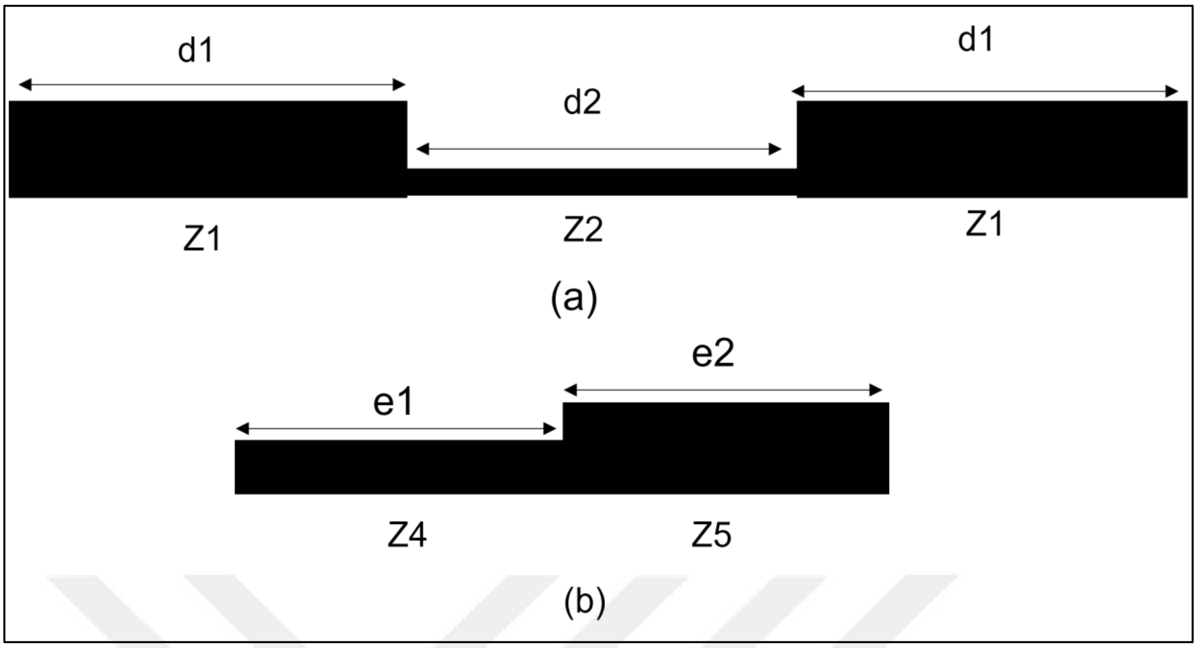

Figure 2.4: (a)SSIR Step Impedance Resonator, (B) ASIR Step Impedance Resonator.

The SIR arrangement relies on both odd and even excitement. The ensuing resonances for odd-even and excitations can be easily observed under the circumstances of Yin= 0 [36].

(a) Odd mode resonance condition:

$$tan\ \theta_0 tan\ \theta_s = R \tag{2.19}$$

(b) Even mode resonance condition:

$$\frac{1}{2R1}\left[1+\frac{G2}{R}\right]\left[\frac{G0}{R1}+\frac{G1}{R2}\right]+\left[G3+\frac{G4}{R}\right]\left[\frac{1}{R1}+\frac{G5}{R2}\right]=0 \tag{2.20}$$

When the parameters are determined by the following:

$$R = \frac{Z_0}{Z_s}, R1 = \frac{Z_1}{Z_s}, R2 = \frac{Z_2}{Z_s}, G0 = \tan\theta_1, G1 = \tan\theta_2,$$
$$G2 = \tan\ \theta_0 \tan\ \theta_1, G3 = \tan\ \theta_s, G4 = \tan\ \theta_0, G5 = \tan\ \theta_1 \tan\ \theta_2 \quad (2.21)$$

Based on (Figure 2-5) then Eqs, the quality (Fr) for odd mode, as well as even mode, is hypothesized using Eqs.(2.22), individually.

$$Fr\ \left[G4 + \frac{G3}{R}\right] - \frac{1}{\pi ZsR} + \frac{G3G4}{\pi Z_s R^2} = 0 \quad (2.23)$$

$$\text{Fr}\left[2R1\left(\frac{G5}{R2} - \frac{1}{R1}\right)(1 - RG0G3) + \left(\frac{G0}{R1} + \frac{G1}{R2}\right)(G3 + RG4)\right]$$
$$+ \frac{1}{2\pi Zs}\left(\frac{G0}{R1} + \frac{G1}{R2}\right)\left(\frac{G3G4}{R} - 1\right) + \frac{R1}{\pi Zs}\left(\frac{G5}{R2} - \frac{1}{R1}\right)\left(G3 + \frac{G4}{R}\right) = 0 \quad (2.24)$$

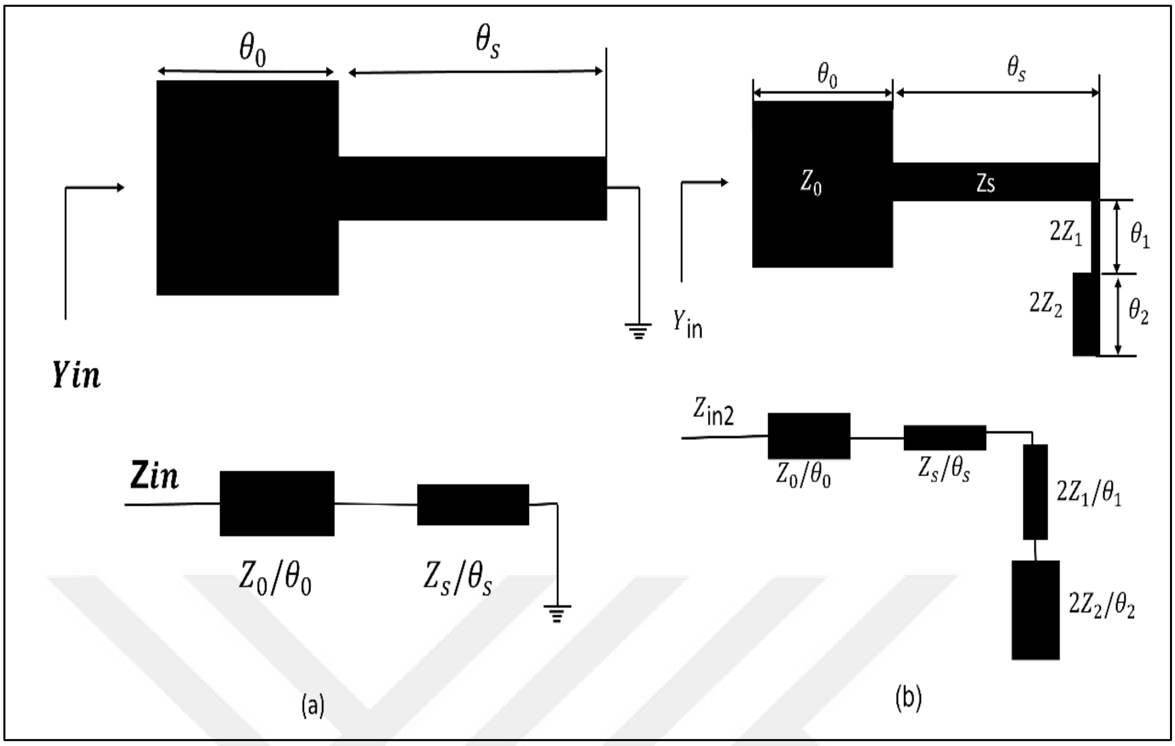

Figure 2.5: Even and Odd SIR Resonance Models.

2.3.4.2 Meander line

Meander-line resonators are planar structures that can be easily fabricated. The wire structure is embedded on a single dielectric substrate, allowing the antenna to be much smaller than it otherwise would be thanks to the microstrip design. Possible low-frequency features, low cost, and simple integration into integrated circuits are the key draws. As a result, they have been included in many devices, such as antennas, filters, couplers, and phase shifters. Basically, the meander line is made up of a single set of equally spaced horizontal and vertical lines joined together to form turns. Actually, the effectiveness of the antenna rises with the number of turns [37]. The resonance frequency of a meander line is also affected by its separation and spacing. The resonant frequency decreases as the latter rises. Similar to this, the resonance frequency falls as meander spacing rises. As can be seen in (Figure 2.6(b)), the impedance in the LC series can be represented in the form of $j(\omega L - 1/\omega C)$, if this is taken into consideration, the meander line resonator's final destination, the phase.

$$\Delta\theta = tan^{-1}\frac{\omega L - \frac{1}{\omega C}}{RL} \quad (2.25)$$

The phase-content meandered-line resonator can be modeled as:

$$\beta = \frac{2\pi}{\lambda_i} \tag{2.26}$$

Where λ_l refers to a measurement of the wavelength at which a resonator operates. This equation follows naturally from the previous ones:

$$\Delta\theta = \beta l \tag{2.27}$$

Or

$$l = \Delta\theta/\beta = \frac{\lambda i}{2\pi}\tan^{-1}\frac{\omega L - \frac{1}{\omega C}}{\text{RL}} \tag{2.28}$$

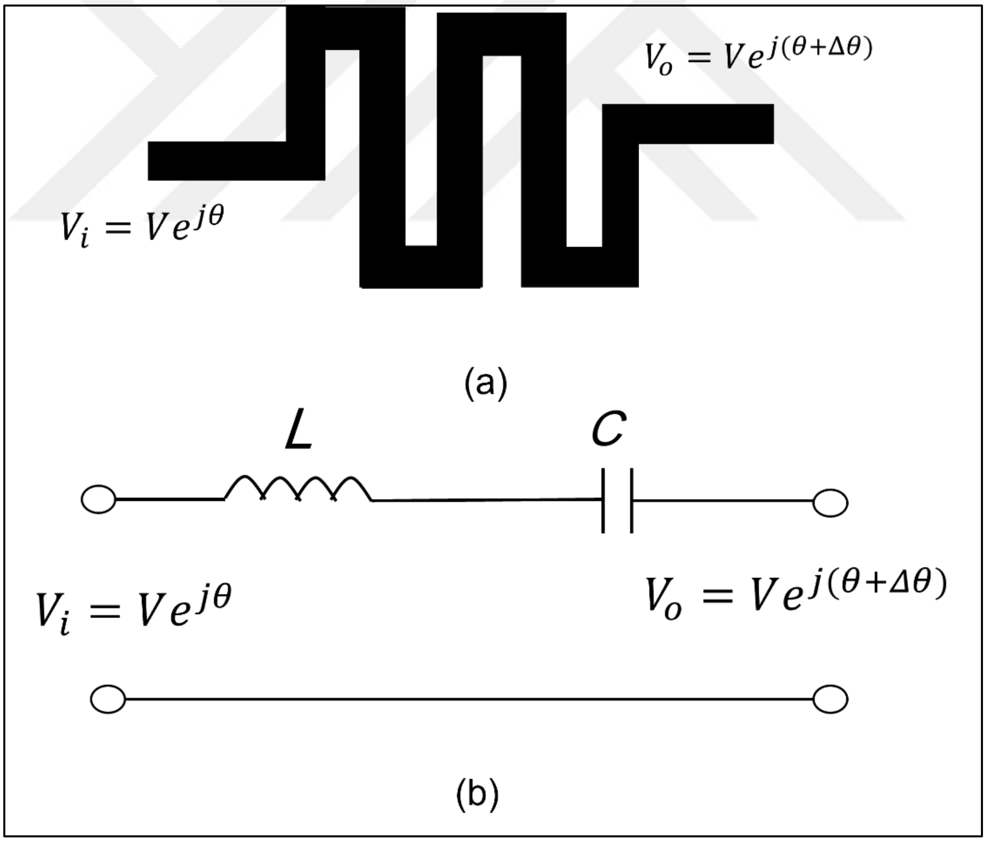

Figure 2.6: (a) Represent the Conventional Design of a Meandering Line Resonator; (b) The LC of a Meandered Line Resonator.

2.3.5 Filters

In filter design, the frequency response is frequently examined as it constitutes the filter's fundamental characteristic. As shown in filters are usually grouped into four types:

a. Low pass filter
b. High pass filter
c. Bandpass filter
d. Band stop filter (notch).

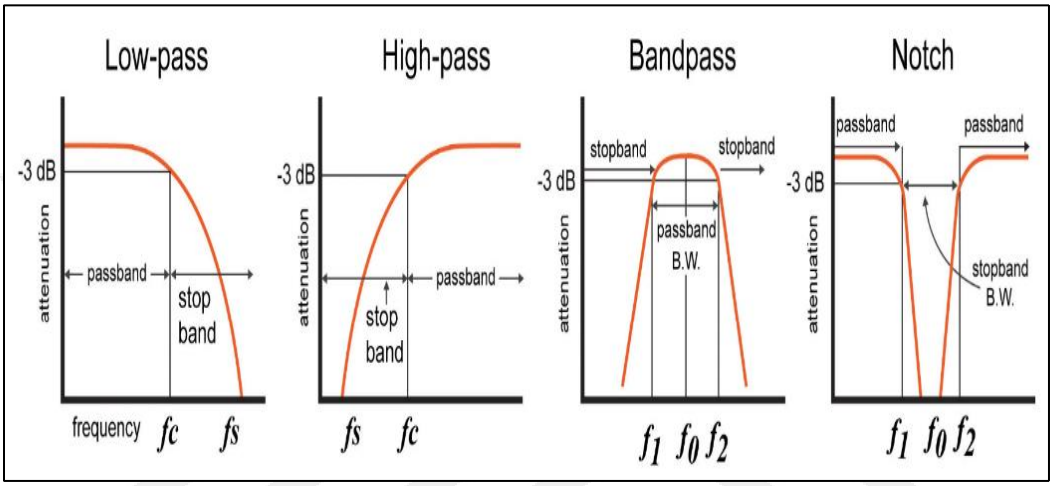

Figure 2.7: Types of Filters [38].

Band-pass filters and diplexers are the main elements in many modern wireless communication systems. Due to the advantages of these circuits, they are a popular choice in radio transmission, radar systems, satellite communication systems, and broadband wireless communication. As seen in (Figure 2.8), an analog bandpass filter is a two-port network that may be characterized in terms of the scattering parameter known as the S-parameter. A band-pass filter only allows frequencies within a given band; frequencies outside of that band are rejected. To illustrate, a band-pass filter that attenuates all frequencies outside of a specified range. The range is established using the fundamental frequency (F0) and the bandwidth (BW), both of which are expressed in hertz (Hz). Band-stop filters, often called notch filters, play a crucial function in blocking off noise while allowing the required signal through. A filter is implemented as a series of resonators that are electromagnetically linked to one another and are connected to an external feed connection. The overall output of the device is determined by the number of couplings between the resonators as well as the kind of couplings [39] [40]. Traditional microstrip

BSF consists of quarter-wavelength long, straight, open-circuited resonators connected by wires of a wave's length in length [27].

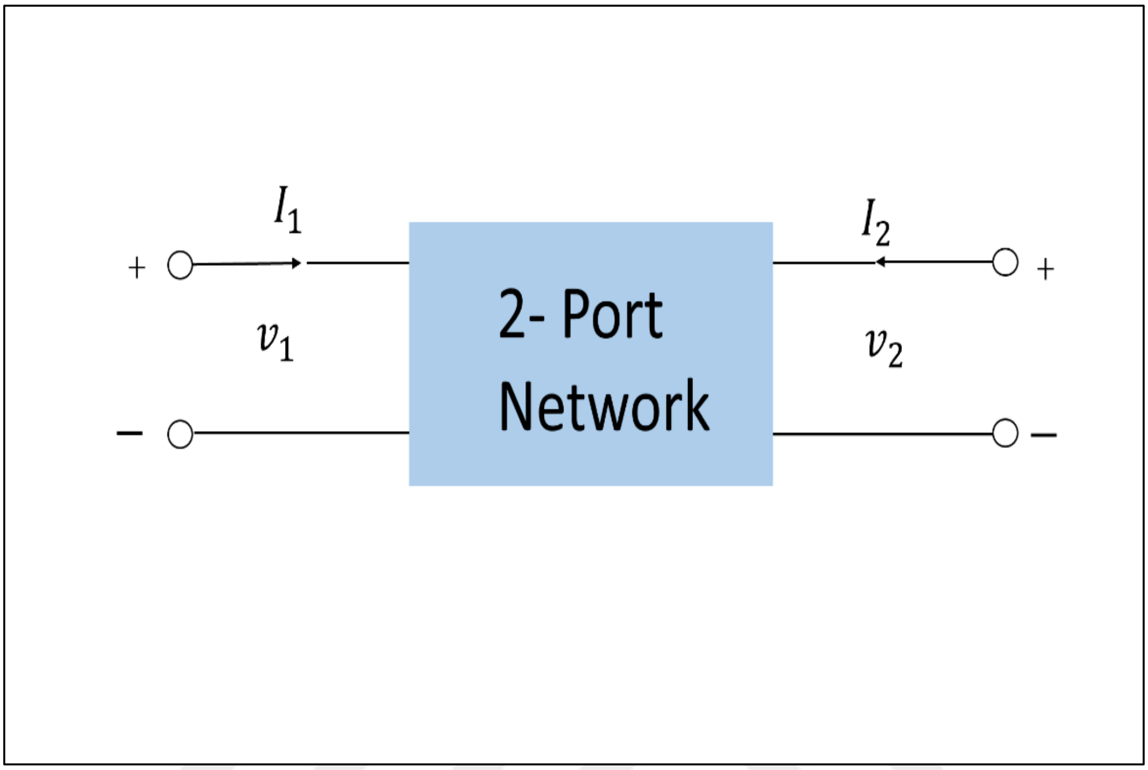

Figure 2.8: S- Parameter.

The filter response is characterized by its transfer function, which is used in the microwave range to provide the required expression to the transmission coefficient $S_{21} = |S_{21}|e^{-i\emptyset_{21}}$. Which characterizes the filter's response. The group delay (τ_D), which represents the cumulative delay of a filtered signal, is a crucial parameter that determines the filter properties. group delay (τ_D),

$$\tau_D = \frac{d_{\emptyset_{21}}}{d\omega} \tag{2.29}$$

Where ϕ_{21} is in radians ω and is in radians per second. In many realistic implementations, however, the filter requirements are mainly about the amplitude function $|S_{21}|$ | (or $|S_{21}|$ for a reciprocal network) that explains how the response magnitude varies with the frequency. This is also achieved through the response of the so-called insertion loss (IL), described as [39] [41]:

$$IL|_{dB} = 10\log\left(\frac{p_{\text{inc}}}{p_{\text{Tran}}}\right) = 10\log\left(\frac{1}{|S_{21}|}\right) = -|S_{21}|_{dB} \tag{2.30}$$

In the two-port network where p_{inc} and p_{Tran} are incident and transmitted power respectively. In the case of the ideal as seen in (Figure 2-9(a)), a filter displays a completely rectangular response of the amplitude, where $s_{21} = 0$ is within the passband and $-\infty$ is elsewhere. In fact, the phase as just a function of frequency would be linear, indicating a consistent delay across the band. Forefront such conditions would precisely reproduce the input spectral components present in the passband in the output signal, whereas the spectral information outside the passband would be entirely reflected. Since it is impossible to realize this ideal filter, a small but finite passband insertion loss IL_{BW} is always found in real cases as in (Figure 2.9(b)) [41].

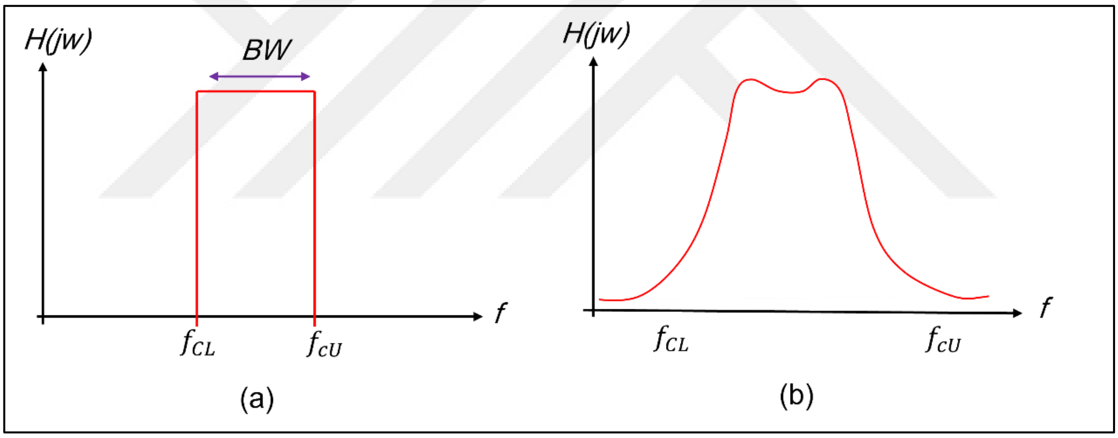

Figure 2.9: (a)Ideal Filter Amplitude Response. (b)Real Filter Amplitude Response.

The flowchart shown in (Figure 2.10) explains the progress of filter implementation.

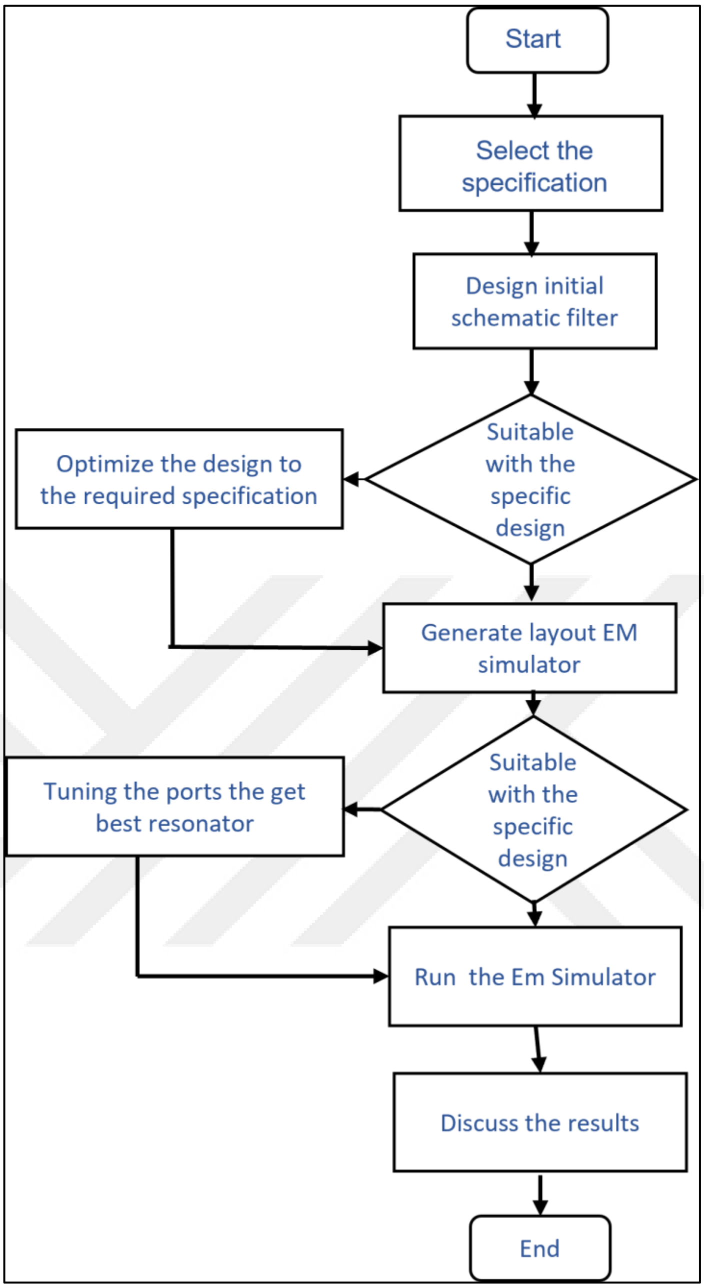

Figure 2.10: Progress of Filters.

2.3.5.1 LC Circuits

An inductor (L), as well as a capacitor (C) coupled in series, form a passive circuit known as an LC circuit. The operation of the circuits is influenced by the additional resistance that is there constantly. These circuits are used to create singles at particular frequencies or to receive signals from more complicated signals at particular frequencies. The π −equivalent circuits can produce a high and low-impedance lossless connection terminated at both ends by comparatively low-impedance lines shown in (Figure 2.11).

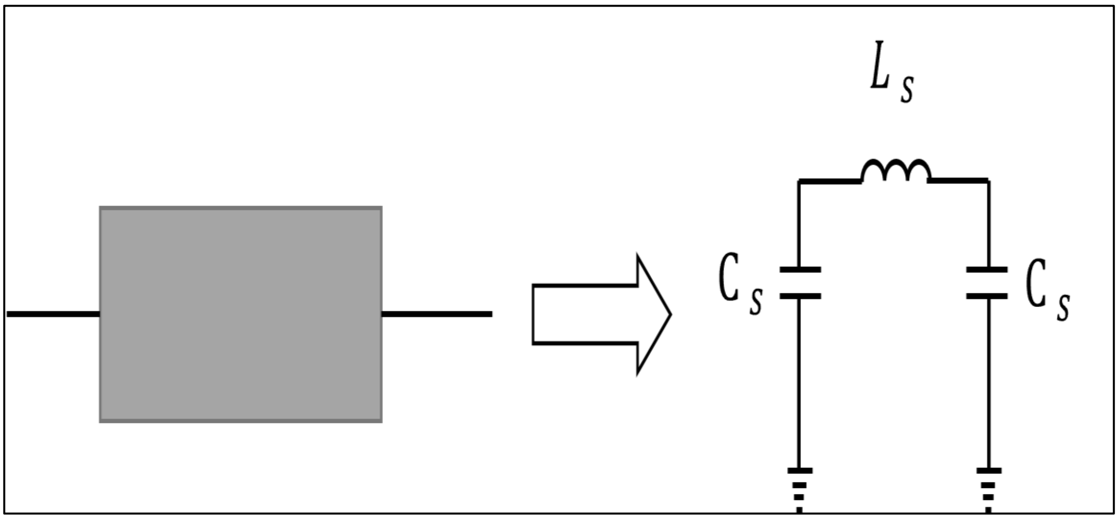

Figure 2.11: Configuration and LC Circuit Equivalent of a High and Low Impedance Lossless Line.

The following formula may be used to determine the values of inductors and capacitors.

$$L_S = \frac{1}{\omega} \times Z_S \times \sin\left(\frac{2 \times \pi}{\lambda_g} l\right) \tag{2.31}$$

$$C_S = \frac{1}{\omega} \times \frac{1}{Z_S} \times tan\left(\frac{\pi}{\lambda_g} l\right) \tag{2.32}$$

The physical microstrip line length is represented as l, and the characteristic impedance is Z_s , the guided wavelength at center frequency is λ_g , and the effective permittivity is ε_{re}, which may be calculated with the help of equations.

As can be seen, the formulas of bend have been examined. Microstrip bends can be indicated through the equivalent network as shown in (Figure 2.12). The following closed-form formulas are used to calculate capacitance and inductance which are provided by Gupta et al, [42].

$$\frac{c}{w}\left(\frac{pf}{m}\right) = \begin{cases} \frac{\left(14\varepsilon_r + 12.5(w/h) - (18.3\varepsilon_r - 2.25)\right)}{\sqrt{w/h}} + \frac{0.02\varepsilon_r}{w/h}\frac{w}{h} < 1 \\ (9.5\varepsilon_r + 1.25)\frac{w}{h} + 3.2\varepsilon_r\frac{w}{h} > 1 \end{cases} \quad (2.33)$$

$$\frac{1}{h}\left(\frac{nh}{m}\right) = 100\left\{4\sqrt{\frac{w}{h}} - 4.21\right\} \quad (2.34)$$

Where the Butterworth filters equation is given by:

$$C_k = 2sin\left[\frac{(2k-1)}{2n}\pi\right] \leftrightarrow k = odd \quad (2.35)$$

$$L_k = 2\sin\left[\frac{(2k-1)}{2n}\pi\right] \leftrightarrow \mathrm{k} = \text{ even} \quad (2.36)$$

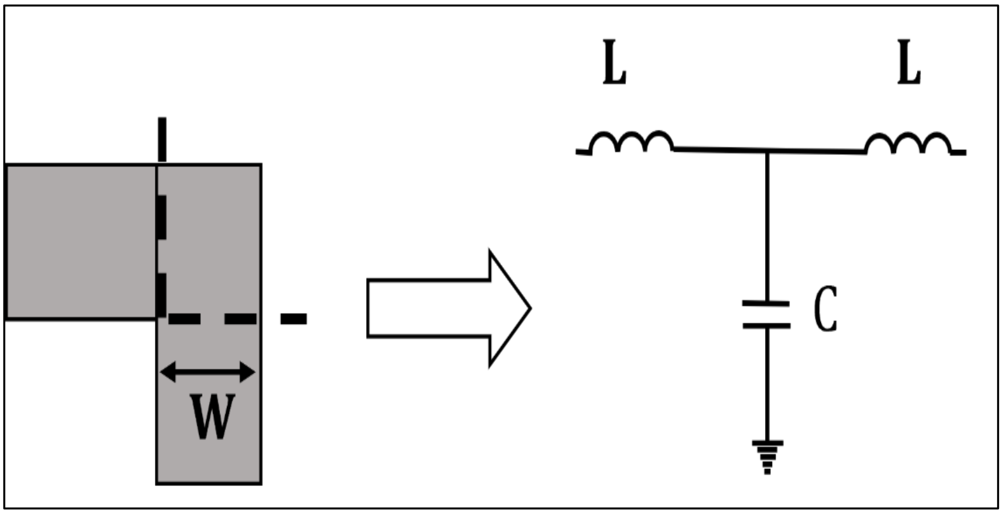

Figure 2.12: Bend's Configuration and Equivalent Circuit.

2.3.5.2 Bandwidth

The term bandwidth is used widely throughout the fields of science and engineering, from the macroscopic to the sub-atomic, and in a wide variety of disciplines, from optics and electromagnetics to imaging and sensing dynamics as well as controls [43]. There are three significant recourses in electronic communication. They are transmitting power, bandwidth, and communication infrastructure. Bandwidth is the frequency or group of frequencies used for transmitting information from the source to the final customers[44]. In addition, A filter's bandwidth is defined as the difference between its highest and lowest passband frequencies. In determining the cut-off frequency, the shape factor is used. This factor is the ratio of the bandwidth measured at two different attenuation levels, like a 2:1 form factor at 30/3 dB. As a result, if we compare the bandwidth measured by both frequency range at 3 dB attenuation to that measured at 30 dB attenuation, we find that the latter is twice as large.

2.3.5.3 Quality factor

(Q) is indeed a ratio of the power flow of the inductor or capacitance to the power rating of the load resistance when the circuit is in resonance. The ratio of stored energy to total energy is also a metric of quality. In order to keep the signal amplitude consistent at the frequency (the resonant frequency), f_r, where the electricity is constant with time, the Q factor is defined as the ratio of energy stored inside the resonant frequency to the energy supplied by the generator per cycle.

$$Q = 2\pi \times \text{ Energy stored/Energy dissipated per cycle} \qquad (2.37)$$

Or

$$Q = 2\pi f_r \times \textit{ Energy stored / Power Loss} \qquad (2.38)$$

Most reverberant systems, whether stray voltage or mechanical, can be described by a second-order differential equation, the coefficients of which can be expressed in terms of the factor 2π leads Q. To begin, the total amount of energy kept in an electrical system's lossless inductors as well as capacitors are referred to as the stored energy. The lost energy, on the other hand, represents the total of the energy that is dissipated as a result of the cycle-long resistance encountered. Second, the sum of a system's kinetic and potential energies at a given instant is called its stored energy, or the max number that can be stored, in a mechanical system. The cost of maintaining amplitude via an outer conservative force is the energy dissipated during each cycle.

With respect to large Q, values, the following equation is presented mathematically:

$$Q = \frac{f_r}{\Delta f} = \frac{\omega_r}{\Delta \omega} \tag{2.39}$$

In this expression, Δf represents the bandwidth, f_r is the resonant frequency, $\Delta\omega$ is the angle BW, as well as $\omega r = 2\pi f_r$ is the angle resonant frequency.

3. DIPLEXER DESIGN

3.1 INTRODUCTION

Many scholars in the field of wireless communication have proposed different structures for the design of diplexers to come up with efficient results. The ability of the microwave diplexer to combine two separate filters into one device via communication channels has generated a great deal of interest in its design. In this study, compact microstrip diplexers based on meander line resonators, uniform impedance resonators, and step impedance resonators have been developed using FR4 epoxy laminate material. The introduced structure has a simple topology, compact circuit size, and high isolation between the output ports are achieved. Therefore, these characteristics are suitable for wireless applications. In this chapter, the proposed diplexer is introduced and analyzed.

3.2 DESIGN THEORY

The conventional method for creating a diplexer begins with the construction of two bandpass filters with distinct passbands. After that, it is necessary to combine them with a compatible network. This portion of the circuit is crucial to the design process.

3.3 FILTER DESIGN

In general, the microstrip diplexer design process begins with the design of two band-pass filters. The suggested architecture for the microstrip band-pass filters is illustrated in (Figure 3.1) and (Figure 3.2). As is evident, this structure comprises a meandering line resonator, step impedance resonators SIR and UIR and patch, and two input/output feed lines.

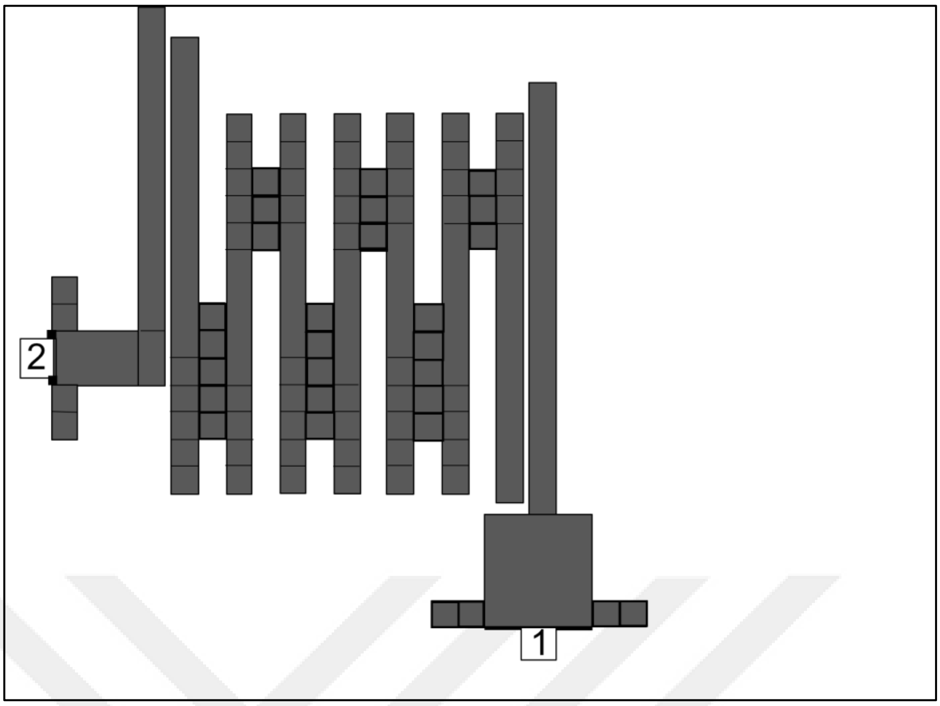

Figure 3.1: First Bandpass Filter.

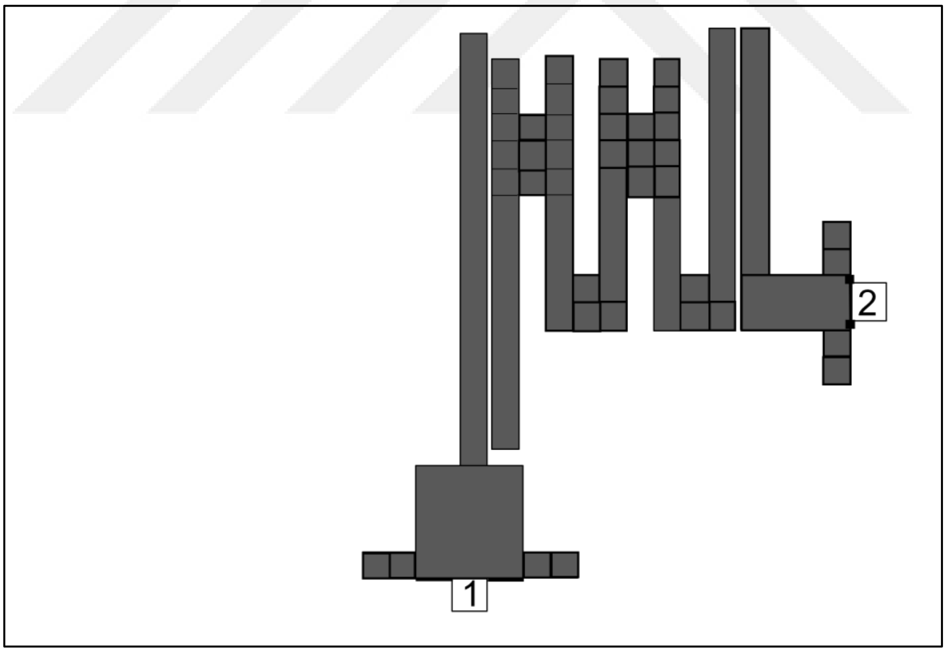

Figure 3.2: Second Bandpass Filter.

3.4 DIPLEXER DESIGN

The diplexer is designed based on the equivalent LC circuit; the LC circuit is displayed in (Figure 3.3).

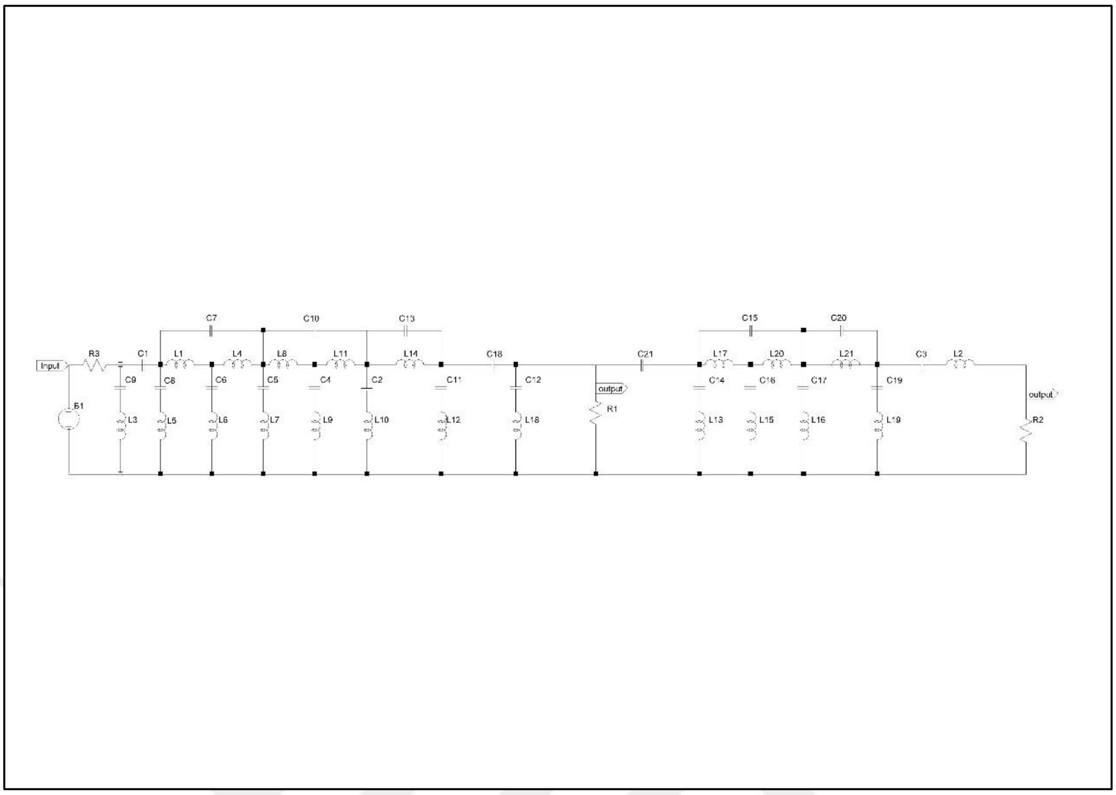

Figure 3.3: The LC for Diplexer.

The fundamental idea for designing a diplexer begins with applying two bandpass filters operating at different passbands. The proposed structure contains two transmission lines and input/output feed lines and is tuned to operate at the desired resonant frequencies. In addition, it contains UIRs and SIRs that gain a lot of recognition due to their affordability and simple topology SIR was tuned to the middle frequency of the band that was wanted. As can be seen, SIRs have less size than uniform impedance resonators (UIR). The dimensions and the SIR position relative to the feed lines are different from one filter to another. The SIR is made up of alternating narrow and wide signal line sections in which the impedance of the narrow parts is much greater than that of the wide sections of the line. In addition, the consists proposed structure of a meander line resonator. Conceptually, this resonator can be made by folding a straight-line resonator into a meander-line resonator, as shown in Each resonator is made from a series of N turns. Therefore, the band-pass filter's resonant frequency can be changed by changing the number of turns or the length of each turn. If the feed lines and the meander line resonator are set up well, the meander line resonator can make the circuit smaller and give it better electrical performance. This reduction in size may be explained by the suggested filter's slow-wave effect. Finally, the meander line can be defined as consisting of a single set of horizontal and vertical lines with identical spacing that are linked to produce turns. The effectiveness of the antenna rises with the number of turns.

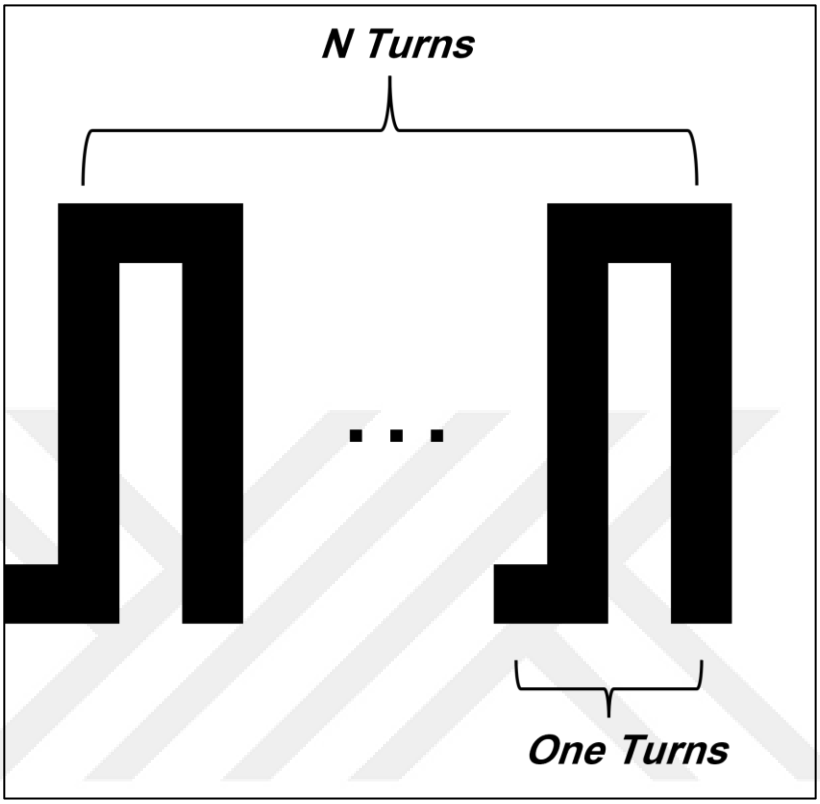

Figure 3.4: The Arrangement of the Meandering Line Segments.

3.4.1 Design Specification

The proposed diplexer filters have several specifications as shown in Table 3-1.

Table 3.1: Information About the Planned Diplexer Filters' Technical Details.

Specifications	Proposed design
Materials (substrate)	FR4
Dielectric constant	4.3
TanD	0.02
Thickness (mm)	1.5
FBW1, FBW2	5%, 5.9%

Technology	SIR, UIR, Meander line
Application	GSM-II, WIFI/WLAN
F1, F2 (GHz)	1.94 GHz, 2.515 GHz
Order	3
Response	Butterworth

The AWR was employed in the destining and simulating of the proposed microstrip diplexer. The microstrip diplexer has an intended overall substrate size of $32 \times 26\text{mm}^2$, and was built on an FR4 substrate. This substrate features a 1.5 conductor thickness, a 1.5 mm thickness, a loss tangent of 0.02, and a relative dielectric constant of 4.3. This design was based on the equivalent circuit by Butterworth and the optimizer tools of the AWR simulator. The microstrip diplexer was designed to function under frequency channels of 1.94 GHz and 2.515 GHz, with highly feasible band isolation and tolerable frequency responses. Instead of combining two filters, additional ports, or other associated devices, the obtained size reduction is achieved through the integration of two filters into a single device. (Figure 3.5) illustrates the proposed diplexer based on the meander resonators, SIR, and UIR elements before assembling. SIR elements are primarily found around SMA connectors and the higher ends of input/output feeders. In fact, when the two filters are combined, the required frequency response is weakened. Therefore, proper optimization of each component in the circuit is necessary. The resonant frequency of the filter is controlled by the number of turns, the length, and UIR and SIR elements.

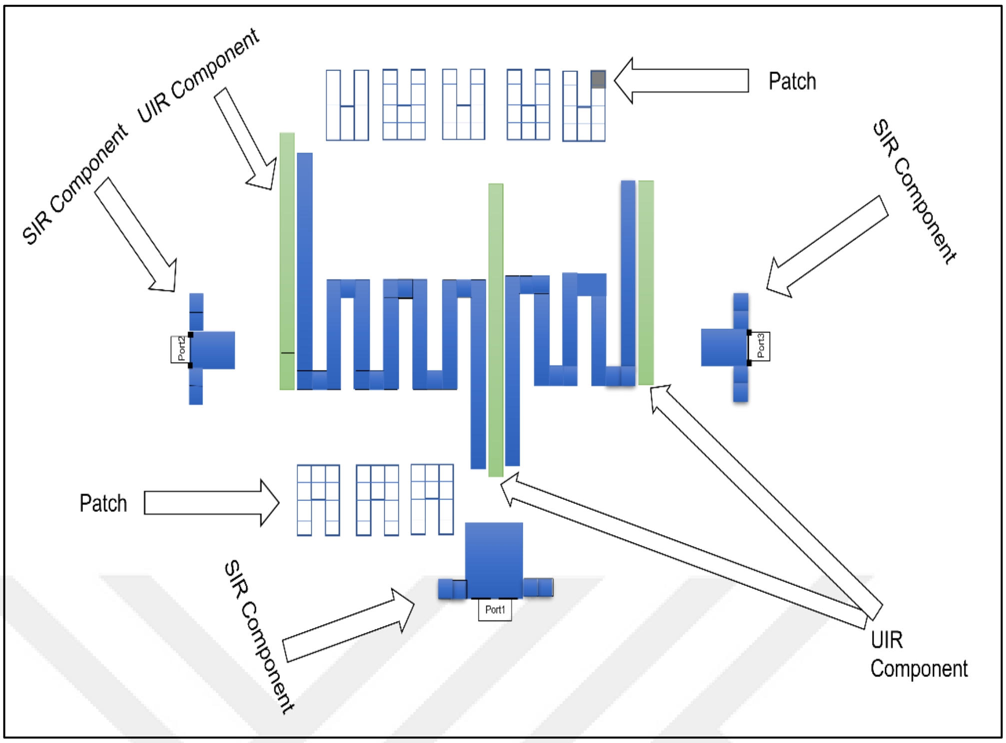

Figure 3.5: Suggested Diplexer Components Before Assembly.

The proposed diplexer which contains a meander line resonator, SIRs, and UIRs, has dimensions as follows in Table 3.1:

Table 3.2: Diplexer Dimensions.

Parameters	L1	L2	L3	L4	L5	L6	L7	L8	L9
Dimension	2	9.2	5	1	4.2	16	9.4	9.8	12
Parameters	W1	W2	W3	W4	W5	G1	G2	G3	
Dimension	3	1	3	1	4	0.2	0.6	0.4	

The diplexer dimensions (in mm units), as it is shown in (Figure 3-6).

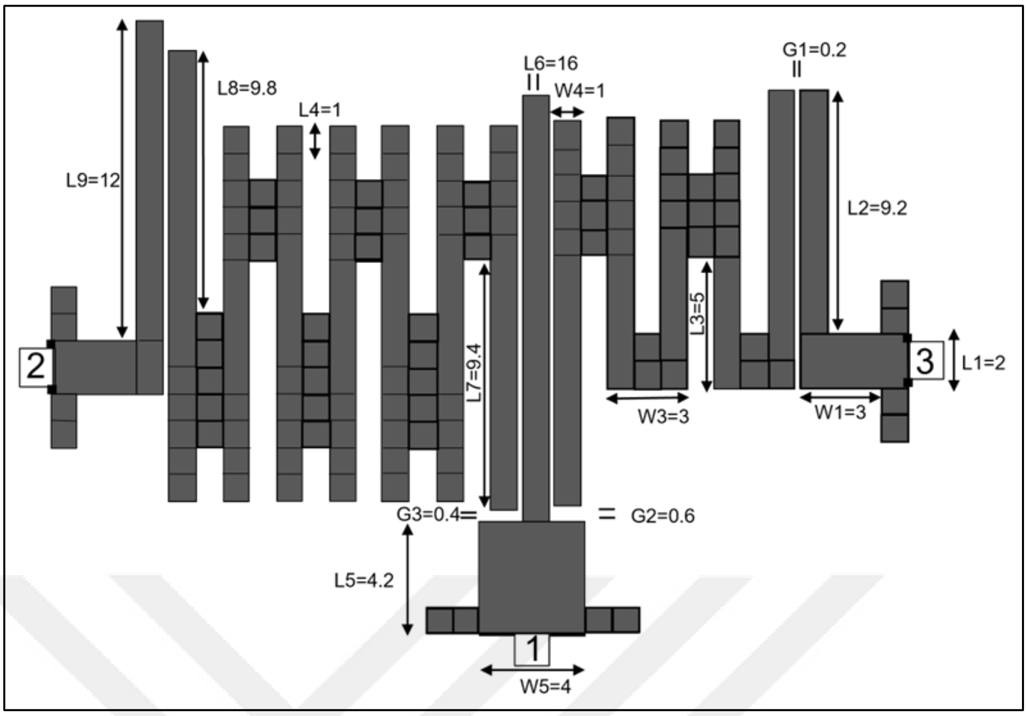

Figure 3.6: The Dimensions of the Proposed Diplexer.

4. RESULTS

4.1 INTRODUCTION

This chapter presents the simulation of the proposed diplexer that can be used in different wireless communication systems due to its compact size and affordable price. From the proposed design, excellent performance characteristics including high isolation, low insertion loss, and good frequency selectivity are all achieved. The proposed design has been created and stimulated using Advanced Wave Research (AWR). The fabrication of the proposed diplexer using FR4 substrate was checked through the use of VNA (Vector Network Analyzer).

4.2 EQUIVALENTS CIRCUIT MODELS

The values of the proposed design's microstrip parameters, inductors, and capacitors have been indicated using the Butterworth equations from ((2.31)-(2.36)); Through (Figure 4.1) using the LT spice program, the LC circuit for the proposed diplexer is depicted. The computed values for the LC circuit component are displayed in (Table 4.1). Through the outcome of the EM simulation, it has been observed that both are quite similar.

Table 4.1: LC Circuit Component Value.

Capacitance	Value (pF)	Inductance	Value(nH)
C_1	1p	L_1	5.3n
C_2	0.6p	L_2	2n
C_3	1p	L_3	0.1n
C_4	0.6p	L_4	5.3n
C_5	0.6p	L_5	0.1n
C_6	0.6p	L_6	0.1n
C_7	0.001p	L_7	0.1n

C_8	0.6p	L_8	5.3n
C_9	0.6p	L_9	0.1n
C_{10}	0.001p	L_{10}	0.1n
C_{11}	0.6p	L_{11}	5.3n
C_{12}	0.6p	L_{12}	0.1n
C_{13}	0.001p	L_{13}	0.2n
C_{14}	1.3p	L_{14}	5.3n
C_{15}	0.005p	L_{15}	0.2n
C_{16}	1.3p	L_{16}	0.2n
C_{17}	1.3p	L_{17}	6n
C_{18}	0.4p	L_{18}	0.1n
C_{19}	1.3p	L_{19}	0.2n
C_{20}	0.005p	L_{20}	6n
C_{21}	0.4p	L_{21}	6n

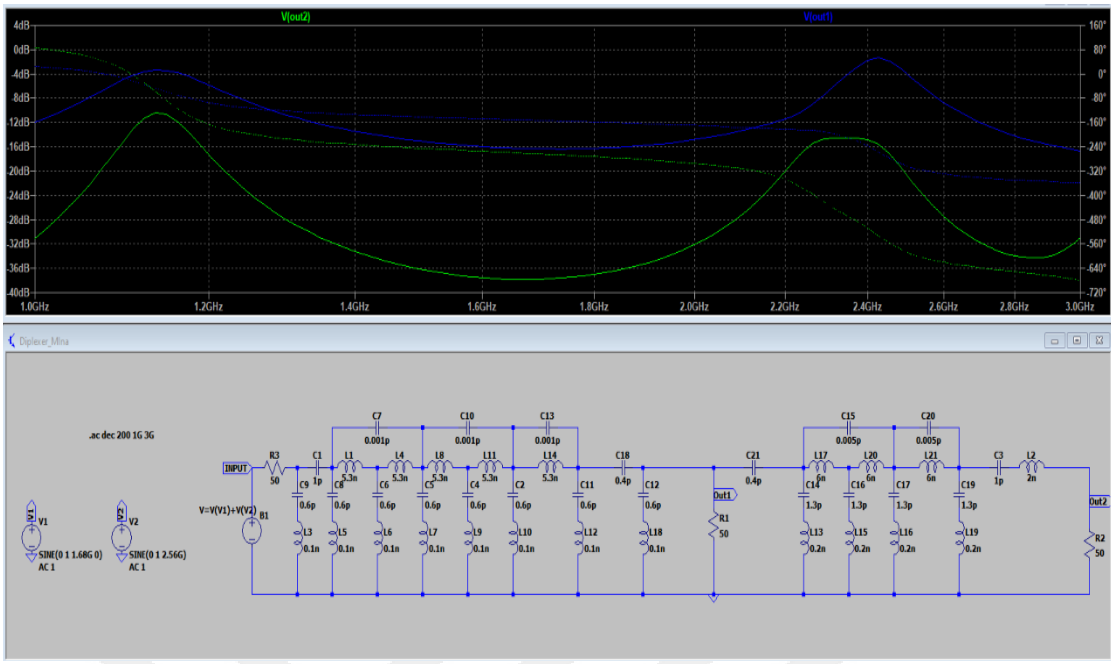

Figure 4.1: Equivalent LC Circuit of the Proposed Diplexer.

4.3 SIMULATION RESULTS

The outcomes of the suggested diplexer are displayed in (Figure 4.2). The proposed design has a return loss (RL) of 31.69 dB and an insertion loss (IL) of 2.92 dB. In addition, the transmission channel (Tx) of the first frequency band has a bandwidth between 1.892-1.988 GHz with a 1.94 GHz central frequency with fractional bandwidth of 5%. On the other hand, the receiving channel (Rx) of the second frequency band has a bandwidth that ranges from 2.445 GHz to 2.598 Gigahertz, with a central frequency of 2.515 GHz with ΔF of 6%, and has insertion and returns loss of 2.51 dB and 29.26 dB respectively. According to simulation results, the recommended configuration maintains an isolation of over 25.2 dB between the two filters.

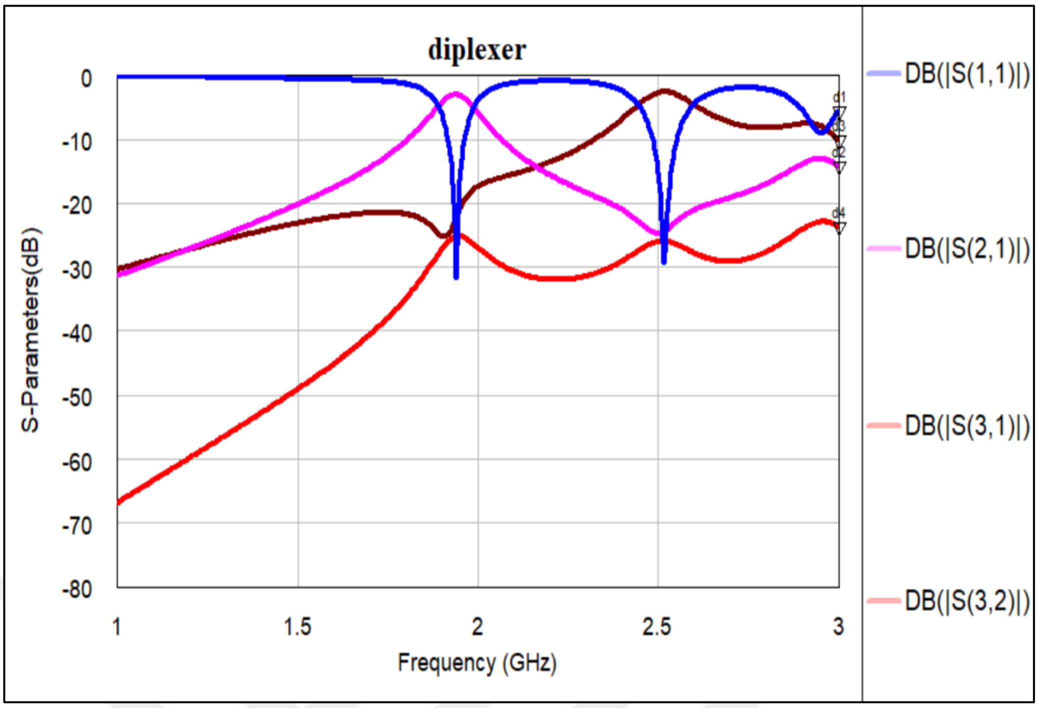

Figure 4.2: The Simulation Outcomes for The Diplexer Built on an FR4 Material Substrate.

4.3.1 Group Delay Using (AWR)

The performance of the group delay for the scattering parameters S11, S21, S31, and S32 is displayed in (Figure 4.3). The GD measurement determines the average filter delay with respect to frequency. When the group delay has a negative value, it reflects that the diplexer forecasts the pulse's position at a later time using its current location. In other words, negative group delay represents a signal delay and is a significant parameter to consider in the design of the diplexer and received considerable attention in the field of RF microwave systems. The GD values are listed in Table 4.2 below:

Table 4.2: Group Delay Values.

S-parameter	Frequency (GHz)	Group delay (ns)
s_{11}	1.94 2.515	-36.65 -29.94
s_{21}	2.5	-1.052
s_{31}	1.91	-2.432
s_{32}	2.701	0.2694

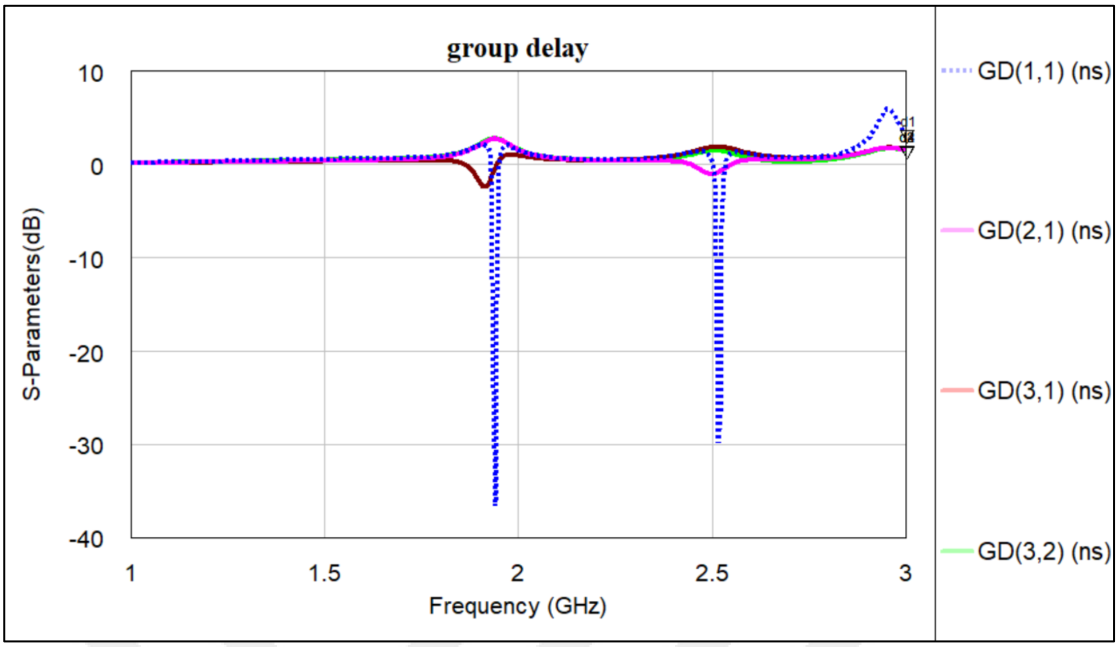

Figure 4.3: The GD Results for Various Scattering Parameters.

4.3.2 Phase Response Using (AWR)

The phase response of the final diplexer design for all S parameters is presented in (Figure 4.4). As an illustration, the phase response that shows the correlation between the phase of a sinusoidal input and the resulting output signal is a trait present in all devices that receive an input and produce an output signal, such as amplifiers or filters.

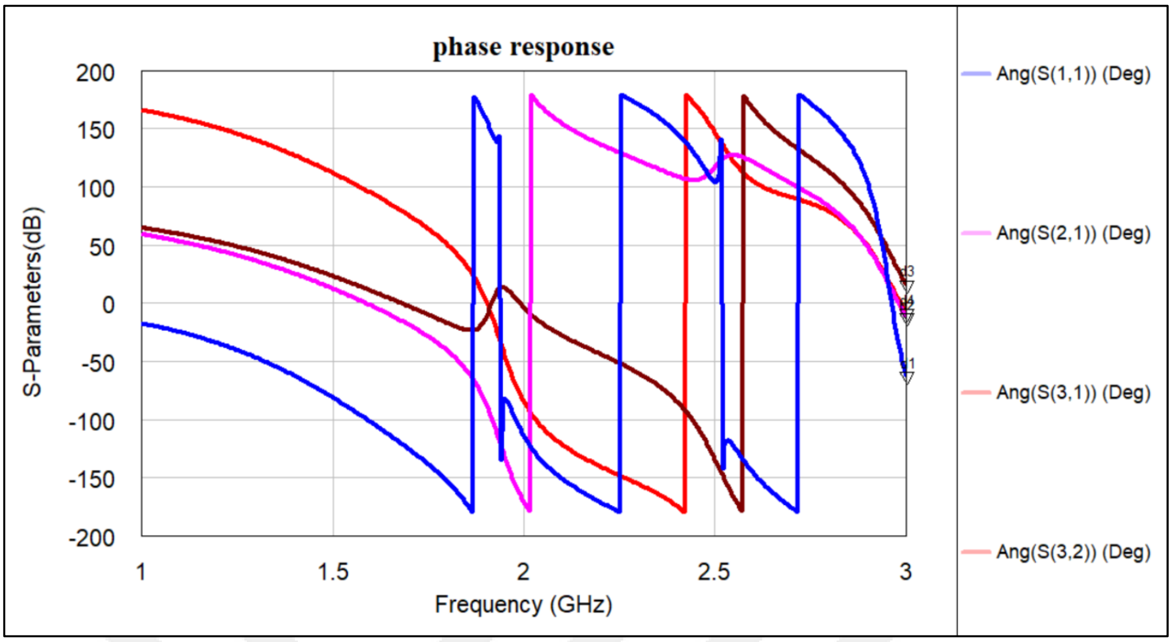

Figure 4.4: Phase Response of the Designed Diplexer for All S Parameters.

4.4 FABRICATION AND EXPERIMENTAI RESULT

The prototype diplexer that was constructed and simulated in this chapter has been fabricated using an FR4 substrate with a 1.5mm thickness and 32×26mm^2 dimensions. The fabrication has been done in the laboratory with Printed Circuit Board (PCB) companies. The prototype specifications and parameters are compliant with the constraints of the proposed standard. A VNA (Vector Network Analyzer) was type VNA-DL 1-8800 MHz used to evaluate the constructed diplexer, according to (Figure 4.5).

Figure 4.5: Vector Network Analyzer.

4.5 FABRICATION AND MEASUREMENTS

Regarding the fabrication process, firstly, the proposed diplexer which is comprised of two filters has been exported to the printer machine as a Gerber file. To illustrate, the designed diplexer which was determined by (AWR) Applied Wave Research, has been applied to the Gerber file. Secondly, the layout layers of the proposed diplexer using the KiCad 2020 are checked before sending it to the factory. Afterward, all layout files should be compressed before being sent to the factory for a quote and payment. After multiple treatments on the substrate material, the Gerber is subsequently uploaded to the machine. (Figure 4.6) depicts the CNC Machine 6090 (router) used to create the suggested design. The layout layers of the diplexer filter front end of manufactured FR4 filters are depicted in (Figure 4.7). The performance of the proposed diplexer has been tested, and design simulations have been validated, using the VNA-DL 1-8800 MHz Vector Network Analyzer. Finally, for measuring the S- characteristics and verifying the performance of produced filters, SMA connections are attached to each of the three ports.

Figure 4.6: CNC Machine 6090 [45].

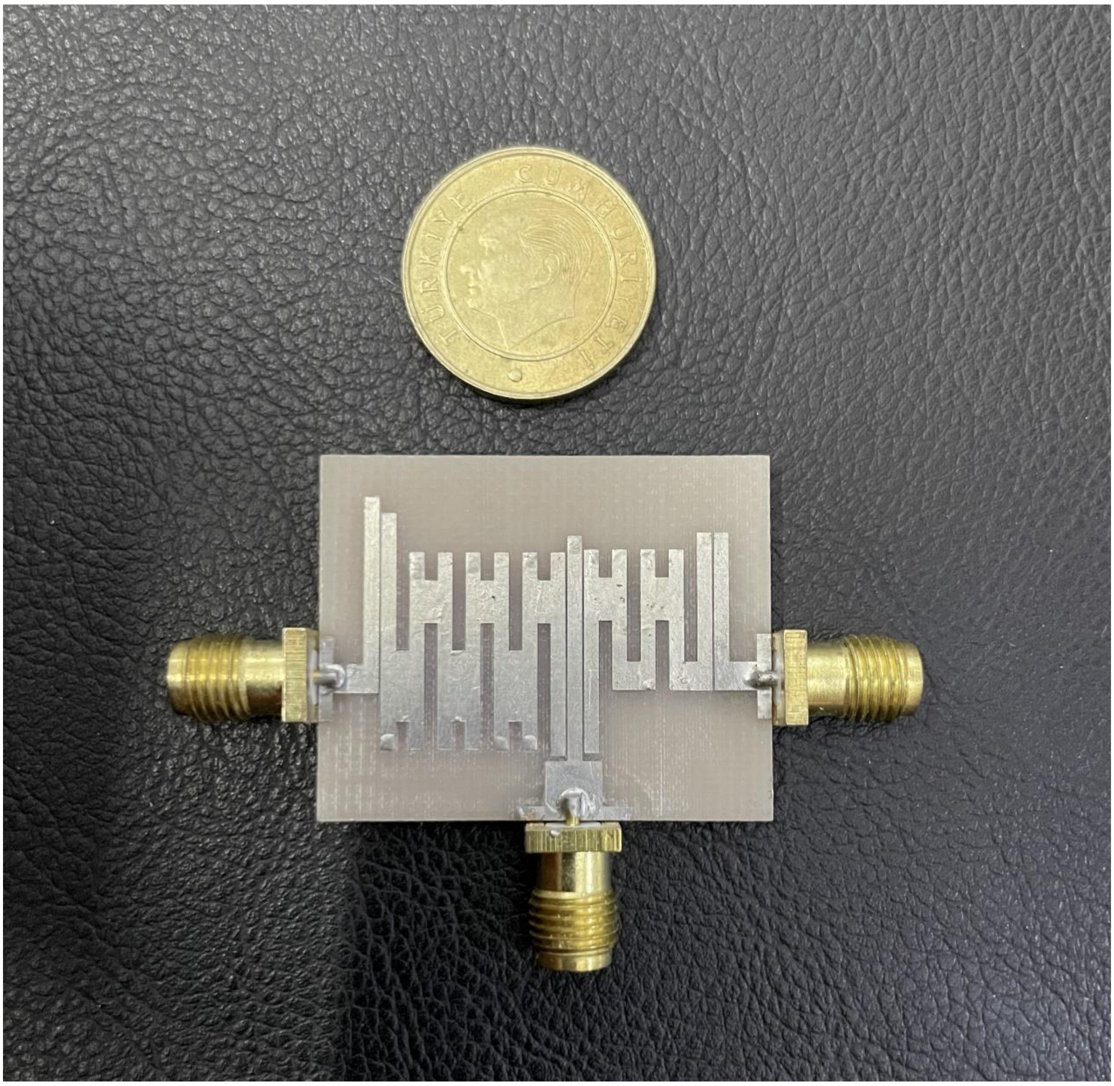

Figure 4.7: Fabricator Diplexer for FR4.

4.6 EXPERIMENTAL TEST AND RESULTS

The constructed diplexer has been attached to Anritsu Vector Network Analyzer for the measurement, after preparing all the criteria for the experimental testing as can be seen in (Figure 4.8). In fact, the constructed diplexer, based on FR4, in order to measure the four parameters S11, S21, S31, and S32. When the measurement is complete, a comparison between the simulation and experimental results is made as illustrated in (Figure 4.9). And as shown in Table 4.3.

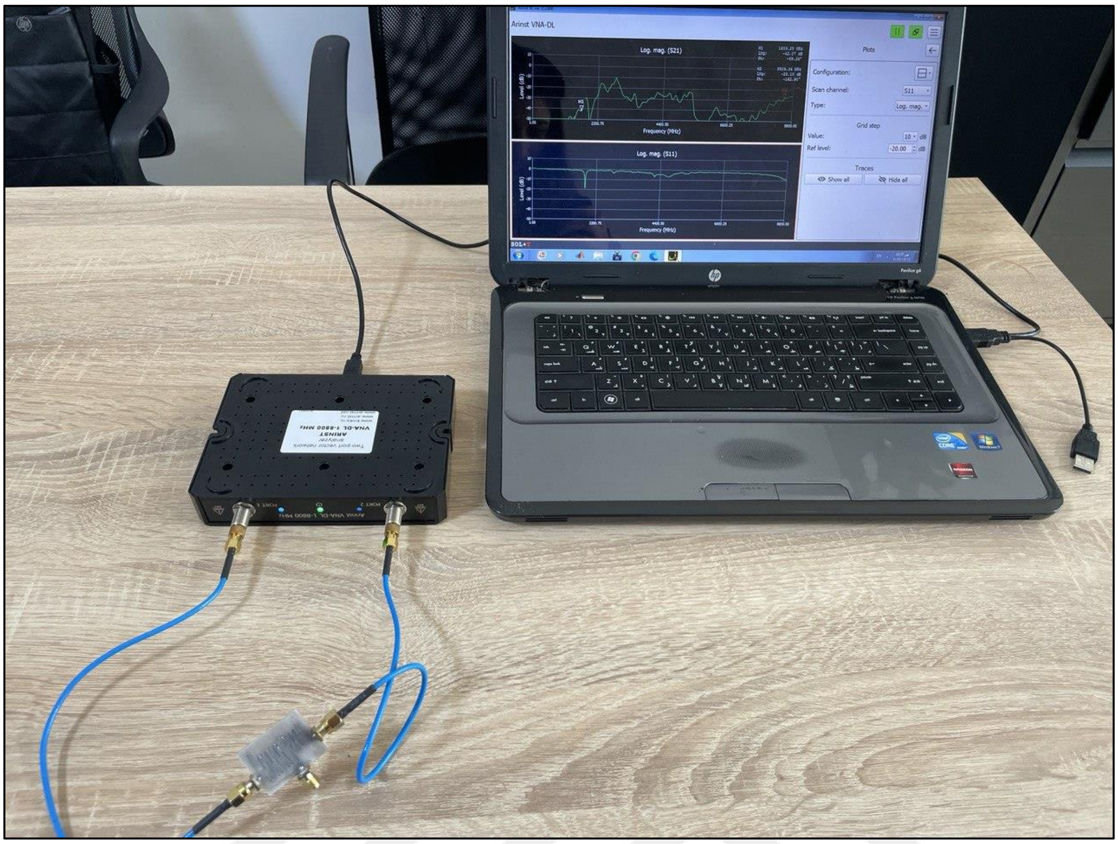

Figure 4.8: Example of Real-Time Diplexer Measuring.

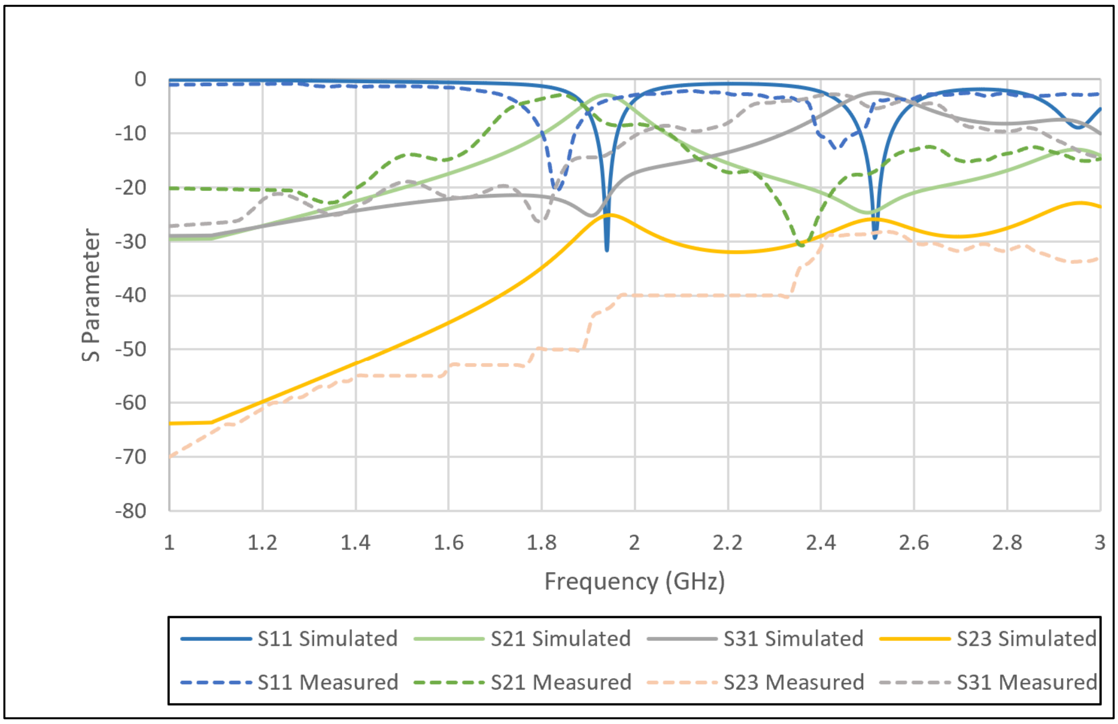

Figure 4.9: Compression Between Simulation and Measurement.

According to the experimental data obtained from the S-parameter measured, the theoretical and

Specifications	Simulation	Measured
Insertion loss	2.9, 2.5	2.9, 3.0
Return loss	31.6, 29.2	20.5, 13.0
Isolation	25.2	26.6

simulation results are superior to the experimental results in terms of response and quality. The strength and purity of the copper alloy used in the production stage may be lower than the usual criteria representing trace conductivity, the substrate material's dielectric constant, and other factors that may have contributed to this downward slope in the outcome. In addition, the connector soldering points (SMA) can have an impact on the filter's overall response, and mismatched connections across the three ports can also affect the response.

Table 4.3: The Suggested Diplexer EM Simulated and Measured Results Comparison.

4.7 COMPARISON WITH PREVIOUS STUDIES

Comparisons between the current study and other relevant studies in the area are presented in Table 4.4. When comparing the results of this investigation to the previous ones, it is apparent that the response rate of the proposed diplexer is much greater. For instance, better return loss and high band isolation. The proposed diplexer has better features compared to previously reported diplexer due to its remarkable compactness which is $32 \times 26\text{mm}^2$. Moreover, the frequency response of the suggested structure demonstrates high selectivity in both passbands. The minor acceptable drawback of the developed device is that its insertion loss for Tx is 2.9 dB and for Rx, it is 2.5 dB.

Table 4.4: Comparison of Results with Previously Published Research.

Reference	Frequency (GHz)	Insertion Loss (dB)	Return Loss (dB)	Isolation (dB)	Size (mm^2)
This work	1.94/2.515	2.9/2.5	31.6/29.2	25	32×26
[46]	1.75/1.95	1.95/1.8	10/12	20	43.5×56.60
[47]	1.580/2.38	2/1.9	17/2	21.5	37×21
[7]	2.6/6	0.6/0.9	11.3/12.4	23.4	25.7×22.3
[48]	2.3/3.5	4.12/2.42	9.58/10.63	--------	105×45
[49]	1.67/1.88	0.43/0.35	16/19.6	22.13	27.5×22.3
[4]	1.8/2.5	2.69/2.81	19.19/15.54	17	47.40×247.06
[50]	1.57/3.35	0.01/0.26	31/16	21.68	0.0018×351.7
[11]	2.88/3.29	0.36/0.44	23/7	23	0.2×0.14
[12]	2.58/2.72	0.85/0.8	15.73/24	20	32×11.1
[51]	2.12/3.94	0.25/0.26	18.45/17.47	24	23.4×16.9
[52]	1.6/2.1	0.1/0.16	33/22	22	40.5×23.7
[53]	1.88/3.56	0.12/0.10	19.2/36	20	15×20.2
[54]	2.4/5.5	1.67/1.58	11.1/13.2	25.8	14.6×10.48
[55]	1.8/2.45	2.05/2.15	15/15	25	50×53
[56]	1.8/2.45	2.2/1.8	17/16	21	20.0×52.0

[57]	2.4/2.6	2.24/3.17	12.4/17.86	15	134 × 68.47
[58]	2.36/5.17	2.3/2.8	-----------	18	61.8 × 34.7
[59]	1/1.6	3/3	15/15	20	93 × 39.9

5. CONCLUSIONS AND FUTURE WORKS

5.1 CONCLUSIONS

Microwave filters and diplexers are used in modern radar, cellular phone, satellite, and wireless communication systems due to their high performance, low loss, high isolation, low cost, and small size. Over the past few decades, numerous methods have been presented for designing high-performance microwave filters and diplexers.

a. The proposed diplexer is successfully tested through manufacturing and measurements after being simulated with dual channels and very narrow bandwidths.
b. In fact, the proposed diplexer is made up using an equivalent circuit that operates in the 1.94 GHz and 2.515 GHz frequency ranges, respectively.
c. The proposed structure contains a meandered line resonator, SIR elements, UIR elements, and two feed lines. With the existence of a modified meander-line resonator, the desired electrical performance has been achieved by modifying the length and the number of turns.
d. The response of the diplexer which is based on an FR4 substrate has been simulated using the Advanced Wave Research (AWR) solver.
e. The suggested design has resulted in a diplexer that can function under 1.94/2.515 GHz resonances for Tx/Rx channels while maintaining isolation of at least 25 dB between the two frequencies.
f. The proposed diplexer may be easily integrated into several wireless designs due to its small size which is $32 \times 26mm^2$ and excellent electrical performance.

The calculated characteristics of the planned circuit show the 1.94 GHz center frequency bandpass filter, (5%) fractional bandwidth, 31.69 dB of return loss, and 2.92 dB of insertion loss.

5.2 FUTURE WORK

In this study, we created a new tiny microstrip diplexer using step impedance resonators (SIRs), uniform impedance resonators (UIRs), and meander-line resonators. Due to its adaptable design, the proposed diplexer can be utilized in numerous wireless communication systems as well as in the domains of industry, science, and medicine. In the future, one of the following lines of investigation could be useful for expanding upon the current findings:

a. The proposed diplexer could be upgraded to triplexers since the diplexer circuit design can easily convert to three channels in order to obtain a three-band of frequencies.
b. The proposed diplexer could be upgraded to dual-band – dual channel to have four bands of frequencies.
c. It is possible to reduce the size of the circuit by changing the dimensions of the meander-line resonator and miniaturizing the filter design.
d. In order to get better insertion loss, the kappa substrate material can be used. This substrate material can be imported from China.

REFERENCES

[1] D. M. Pozar, *Microwave engineering*. John wiley & sons, 2011.

[2] R. J. Cameron, C. M. Kudsia, and R. R. Mansour, *Microwave filters for communication systems: fundamentals, design, and applications*. John Wiley & Sons, 2018.

[3] A. O. Nwajana and K. S. K. Yeo, “Microwave diplexer purely based on direct synchronous and asynchronous coupling,” *Radioengineering*, vol. 25, no. 2, pp. 247–252, 2016.

[4] M. C. Farah and F. Salah-Belkhodja, “A DESIGN OF COMPACT MICROWAVE DIPLEXER IN MICROSTRIP TECHNOLOGY BASED ON BAND-STOP FILTERS USING STEPPED IMPEDANCE RESONATOR,” *Telecommunications and Radio Engineering*, vol. 81, no. 1, 2022.

[5] “https://www.epectec.com/rf-products/diplexers.html”.

[6] R. Levy, R. V Snyder, and G. Matthaei, “Design of microwave filters,” *IEEE Trans Microw Theory Tech*, vol. 50, no. 3, pp. 783–793, 2002.

[7] L. Noori and A. Rezaei, “Design of a microstrip diplexer with a novel structure for WiMAX and wireless applications,” *AEU-International Journal of Electronics and Communications*, vol. 77, pp. 18–22, 2017.

[8] J. R. James, *Handbook of microstrip antennas*, vol. 1. IET, 1989.

[9] H.-W. Deng, Y.-J. Zhao, Y. Fu, J. Ding, and X.-J. Zhou, “Compact and high isolation microstrip diplexer for broadband and WLAN application,” *Progress In Electromagnetics Research*, vol. 133, pp. 555–570, 2013.

[10] S. I. Yahya, A. Rezaei, and L. Nouri, “Design and performance of microstrip diplexers: A review,” *ARO-The Scientific Journal of Koya University*, vol. 8, no. 1, pp. 38–49, 2020.

[11] A. Rezaei, L. Noori, and H. Mohammadi, “Design of a miniaturized microstrip diplexer using coupled lines and spiral structures for wireless and WiMAX applications,” *Analog Integr Circuits Signal Process*, vol. 98, pp. 409–415, 2019.

[12] S. I. Yahya, A. Rezaei, L. Noori, and M. H. Jamaluddin, “Wide Stopband Microstrip Diplexer Using a Novel Configuration for Frequency Division Duplex 2019, pp. 1–5.

[13] Q. Li, Y. Zhang, and C. M. Wu, "Compact and high-isolation microstrip diplexer using distributed coupling feeding line," *Microw Opt Technol Lett*, vol. 60, no. 1, pp. 192–196, 2018.

[14] S. N. Dembele, J. Bao, T. Zhang, and D. Bukuru, "Compact microstrip diplexer based on dual closed loop stepped impedance resonator," *Progress in Electromagnetics Research C*, vol. 89, pp. 233–241, 2019.

[15] S. I. Yahya and A. Rezaei, "A very compact microstrip diplexer fabrication with superior performance for broadband wireless applications," *Microw Opt Technol Lett*, vol. 62, no. 9, pp. 2871–2880, 2020.

[16] A. Rezaei, S. I. Yahya, and M. H. Jamaluddin, "A novel microstrip diplexer with compact size and high isolation for GSM applications," *AEU-International Journal of Electronics and Communications*, vol. 114, p. 153018, 2020.

[17] N. C. Pradhan, K. S. Subramanian, R. K. Barik, and Q. S. Cheng, "Design of a compact SIW diplexer with square cavities for C-band applications," in *2020 URSI Regional Conference on Radio Science (URSI-RCRS)*, 2020, pp. 1–4.

[18] T. Upadhyaya, J. Pabari, V. Sheel, A. Desai, R. Patel, and S. Jitarwal, "Compact and high isolation microstrip diplexer for future radio science planetary applications," *AEU-International Journal of Electronics and Communications*, vol. 127, p. 153497, 2020.

[19] Q.-Y. Lu, Y.-J. Zhang, J. Cai, W. Qin, and J.-X. Chen, "Microstrip tunable diplexer with separately-designable channels," *IEEE Transactions on Circuits and Systems II: Express Briefs*, vol. 67, no. 12, pp. 2983–2987, 2020.

[20] S. I. Yahya, A. Rezaei, and L. Nouri, "The use of artificial neural network to design and fabricate one of the most compact microstrip diplexers for broadband L-band and S-band wireless applications," *Wireless Networks*, vol. 27, pp. 663–676, 2021.

[21] C.-F. Chen *et al.*, "Design of microstrip multifunction integrated diplexers with frequency division, frequency selection, and power division functions," *IEEE Access*, vol. 9, pp. 53232–53242, 2021.

[22] M. M. Shaheen, N. M. Mahmoud, M. A. Ali, M. E. Nasr, and A. H. Hussein, "Implementation of a Highly Selective Microstrip Diplexer with Low Insertion Loss Using Square Open-Loop Resonators and a T-Junction Combiner," *Radioengineering*, vol. 31, no. 3, p. 357, 2022.

[23] D. Ma, K. Zhou, H. Xie, T. Huang, and W. Wu, "Compact or Wide-Stopband SIW Diplexers With High Intrinsic Isolations Based on Orthogonal Dual Modes," *IEEE Transactions on Circuits and Systems II: Express Briefs*, vol. 70, no. 1, pp. 71–75, 2022.

[24] A. Rezaei and S. I. Yahya, "A New Design Approach for a Compact Microstrip Diplexer with Good Passband Characteristics," *ARO-The Scientific Journal of Koya University*, vol. 10, no. 2, pp. 1–6, 2022.

[25] S. Harikirubha, V. Baranidharan, S. Saranya, K. Keerthana, and M. Nandhini, "Different shapes of microstrip line design using FR4 substrate materials–A comprehensive review," *Mater Today Proc*, vol. 45, pp. 3404–3408, 2021.

[26] S. Darlington, "Synthesis of reactance 4-Poles which produce prescribed insertion loss characteristics: including special applications to filter design," *Journal of Mathematics and Physics*, vol. 18, no. 1–4, pp. 257–353, 1939.

[27] J.-S. G. Hong and M. J. Lancaster, *Microstrip filters for RF/microwave applications*. John Wiley & Sons, 2004.

[28] Y. J. Yoon and B. Kim, "A new formula for effective dielectric constant in multi-dielectric layer microstrip structure," in *IEEE 9th Topical Meeting on Electrical Performance of Electronic Packaging (Cat. No. 00TH8524)*, 2000, pp. 163–167.

[29] J. C. Radio, "A new definition of characteristic impedance," 1991.

[30] I. J. Bahl, "A designer's guide to microstrip line," *Microwaves*, pp. 1–380, 1977.

[31] T. C. Edwards and M. B. Steer, *Foundations of interconnect and microstrip design*. Wiley Online Library, 2000.

[32] E. J. Denlinger, "Losses of microstrip lines," *IEEE Trans Microw Theory Tech*, vol. 28, no. 6, pp. 513–522, 1980.

[33] M. V Schneider, "Dielectric loss in integrated microwave circuits," *Bell System Technical Journal*, vol. 48, no. 7, pp. 2325–2332, 1969.

[34] R. Rajni, "A review of Stepped Impedance Resonators in Microwave circuits," in *National Conference on Computing, Communication & Electrical Systems*, 2017.

[35] A. Singh, "Stepped Impedance Resonator and Spiral Resonator Based Metamaterial Unit-Cell.," *Journal of Engineering Science & Technology Review*, vol. 9, no. 3, 2016.

[36] Y. Li, W. Li, and T. Jiang, “Implementation and Investigation of a Compact Circular Wide Slot UWB Antenna with Dual Notched Band Characteristics using Stepped Impedance Resonators.,” *Radioengineering*, vol. 21, no. 1, 2012.

[37] N. Zalfani, S. Beldi, S. Lahouar, and K. Besbes, “A miniaturized planar meander line antenna for UHF CubeSat communication,” *Advances in Space Research*, vol. 69, no. 5, pp. 2240–2247, 2022.

[38] “https://www.allaboutcircuits.com/technical-articles/an-introduction-to-filters”.

[39] D. M. Pozar, *Microwave engineering*. John wiley & sons, 2011.

[40] A. Bhattacharjee and N. K. Singh, “Design, Fabrication And Analysis of Parallel-Coupled Line Bandpass Microstrip Filter for C-Band Application,” *International Journal of Electrical, Electronics and Computer Engineering*, pp. 51–54, 2012.

[41] A. Namsang and P. Akkaraekthalin, “Microstrip bandpass filters using end-coupled asymmetrical step-impedance resonators for wide-spurious response,” *Progress In Electromagnetics Research C*, vol. 14, pp. 53–65, 2010.

[42] Y. Pourasad and G. Karimi, “Design of ultra compact dual-band bandpass filter using L-shaped resonator,” *Int J Microw Wirel Technol*, vol. 9, no. 3, pp. 493–497, 2017.

[43] A. Mojahed, L. A. Bergman, and A. F. Vakakis, “Generalization of the Concept of Bandwidth,” *J Sound Vib*, vol. 533, p. 117010, 2022.

[44] S. K. Routray, P. Mishra, S. Sarkar, A. Javali, and S. Ramnath, “Communication bandwidth for emerging networks: Trends and prospects,” *arXiv preprint arXiv:1903.04811*, 2019.

[45] “www.amazon.com/CNC-6090-Carving-Woodworking-Engraving/dp/B0BG8H889X”.

[46] S. Choocadee, N. Intarawiset, and S. Tantiviwat, “Compact microstrip diplexer using triple-mode stub loaded resonators,” in *2017 IEEE MTT-S International Conference on Microwaves for Intelligent Mobility (ICMIM)*, 2017, pp. 9–12.

[47] A. Chinig and H. Bennis, “A novel design of an H-shaped microstrip diplexer,” *Journal of Microwaves, Optoelectronics and Electromagnetic Applications*, vol. 16, pp. 966–981, 2017.

[48] M. A. S. Sazali, N. A. Shairi, and Z. Zakaria, “Hybrid Microstrip Diplexer Design for Multi-band WiMAX Application in 2.3 and 3.5 GHz Bands,” *International Journal of Electrical and Computer Engineering*, vol. 8, no. 1, p. 576, 2018.

[49] A. Rezaei, S. I. Yahya, L. Nouri, and M. H. Jamaluddin, "Design of a low-loss microstrip diplexer with a compact size based on coupled meandrous open-loop resonators," *Analog Integr Circuits Signal Process*, vol. 102, no. 3, pp. 579–584, 2020.

[50] S. I. Yahya, A. Rezaei, and L. Nouri, "A novel miniaturized microstrip lowpass-bandpass diplexer using patch and interdigital cells for wireless networks," *AEU-International Journal of Electronics and Communications*, vol. 126, p. 153404, 2020.

[51] A. Rezaei, S. I. Yahya, L. Noori, and M. H. Jamaluddin, "Design and fabrication of a novel compact low-loss microstrip diplexer for WCDMA and WiMAX applications," *Journal of Microwaves, Optoelectronics and Electromagnetic Applications*, vol. 18, pp. 482–491, 2019.

[52] A. Rezaei, S. I. Yahya, L. Noori, and M. H. Jamaluddin, "Design of a novel wideband microstrip diplexer using artificial neural network," *Analog Integr Circuits Signal Process*, vol. 101, no. 1, pp. 57–66, 2019.

[53] M. Hayati, A. Rezaei, and L. Noori, "Design of a high–performance lowpass–bandpass diplexer using a novel microstrip structure for GSM and WiMAX applications," *IET Circuits, Devices & Systems*, vol. 13, no. 3, pp. 361–367, 2019.

[54] Y. Wu, L. Hao, W. Wang, and Y. Yang, "Miniaturized and Low Insertion Loss Diplexer Using Novel Inter-Digital Capacitors and Microstrip Section Inductors," *IEEE Transactions on Circuits and Systems II: Express Briefs*, vol. 69, no. 11, pp. 4303–4307, 2022.

[55] H. Liu, W. Xu, Z. Zhang, and X. Guan, "Compact diplexer using slotline stepped impedance resonator," *IEEE Microwave and Wireless Components Letters*, vol. 23, no. 2, pp. 75–77, 2013.

[56] A. Chinig *et al.*, "Microstrip diplexer using stepped impedance resonators," *Wirel Pers Commun*, vol. 84, pp. 2537–2548, 2015.

[57] N. H. Baba, A. H. Awang, M. T. Ali, M. A. Aris, and H. M. Hizan, "Design of a SIW-based microstrip diplexer using TM010 circular cavity," in *Theory and Applications of Applied Electromagnetics: APPEIC 2015*, Springer, 2016, pp. 71–79.

[58] P.-H. Deng, C.-H. Wang, and C. H. Chen, "Compact microstrip diplexers based on a dual-passband filter," in *2006 Asia-Pacific Microwave Conference*, 2006, pp. 1228–1232.

[59] H.-Y. Chen *et al.*, “Integration Design of Filtering Balun Diplexer with Improved Output Isolation Performance,” in *2022 Asia-Pacific Microwave Conference (APMC)*, 2022, pp. 527–529.